Brno University of Technology
Faculty of Mechanical Engineering
Institute of Machine and Industrial Design

Vysoké učení technické v Brně
Fakulta strojního inženýrství
Ústav konstruování

# The behaviour of grease in EHL contacts of ball bearings

**Ing. Michal Okál**
Author
Autor práce

**prof. Ing. Ivan Křupka, Ph.D.**
Supervisor
Vedoucí práce

Dissertation thesis
Dizertační práce

Brno 2025

# STATEMENT

I hereby declare that I have written the PhD thesis The *behaviour of grease in EHL contacts of ball bearings* on my own according to the advice of my supervisor prof. Ing. Ivan Křupka, Ph.D., and using the sources listed in the references.

.....
Michal Okál

# BIBLIOGRAPHICAL REFERENCE

Okál, Michal. The *behaviour of grease in EHL contacts of ball bearings*. Brno, 2025. 128 p., PhD thesis. Brno University of Technology, Faculty of Mechanical Engineering, Institute of Machine and Industrial Design. Supervisor prof. Ing. Ivan Křupka, Ph.D.

# ACKNOWLEDGEMENT

I would like to express my deepest gratitude to my supervisor, prof. Ing. Ivan Křupka, Ph.D., who guided and supported me throughout my studies. I would also like to extend my thanks to Ing. David Koštál, Ph.D., and to the director of our department, prof. Ing. Martin Hartl, Ph.D., for their support and advice during my studies.

Additionally, I am grateful to my colleagues from the Department of Mechanical and Industrial Engineering for fostering a helpful, friendly, and motivating atmosphere. I especially appreciate my office mates, with whom I shared many memorable experiences.

My greatest thanks go to my family and friends, who have accompanied and supported me throughout my academic journey.

# ABSTRACT

This dissertation focuses on the behaviour of grease components in the elastohydrodynamic (EHL) contact of ball bearings and their ability to form a lubricating film. Although ball bearings are among the most widely used engineering components, there are gaps in the current understanding of grease performance in these applications. The most commonly employed methods to study greases include tribometers in ball-on-disc configuration and tests on actual ball bearings. However, these experimental methods have their limitations: the ball-on-disc configuration significantly simplifies the bearing geometry, and tests on real bearings do not provide direct insight into the contact area. In this dissertation, a combination of these approaches is presented, supplemented by experiments using a ball-on-ring configuration device that replicates realistic contact conditions of a ball bearing. By employing fluorescently dyed grease components and optical methods, it was possible to experimentally investigate the individual grease components and observe their contribution to the formation of the lubricating film under various conditions. Specially formulated greases with the same base oil but different types of thickeners in the same ratio of individual components were used for the tests. The findings from the contact simulators were subsequently verified on actual ball bearings, where the lubrication film thickness in EHL contact was measured using the capacitance method. The results were then compared with current predictive models for the development of normalized film thickness in ball bearings. It was discovered that existing predictive models could not accurately forecast the behaviour of certain types of grease, due to the ability of specific thickeners to contribute to the formation of the lubricating film. A deeper understanding of the lubrication processes of greases in EHL contact in ball bearings will facilitate the more precise development of new greases and the refinement of existing predictive models for normalized lubricating film thickness.

# KEYWORDS

Tribology, Ball bearing, Grease, EHL, Thickener, Base oil

# ABSTRAKT

Tato disertační práce se zaměřuje na chování složek plastického maziva v elastohydrodynamickém (EHL) kontaktu kuličkového ložiska a jejich schopnost tvořit mazací film. Ačkoli jsou kuličková ložiska jednou z nejrozšířenějších strojírenských součástek, existují mezery v současném stavu poznání ohledně fungování plastických maziv v těchto aplikacích. Nejčastěji využívané přístupy ke studiu plastických maziv zahrnují tribometry v konfiguraci ball-on-disk a testy na reálných kuličkových ložiscích. Tyto experimentální metody však mají své nedostatky: konfigurace ball-on-disk značně zjednodušuje geometrii ložiska a testy na reálných ložiscích neumožňují přímý vhled do kontaktní oblasti. V této disertační práci je představena kombinace obou přístupů s domplněním o experiment na zařízení konfigurace ball on ring, který vytváří reálné kontaktní podmínky kuličkového ložiska. Pomocí fluorescenčně obarvených složek plastického maziva a optických metod bylo možné jednotlivé složky maziva experimentálně studovat a sledovat jejich příspěvek k tvorbě mazacího filmu za různých podmínek. Pro testy byla použita speciálně vyrobená maziva se stejným základovým olejem, ale s různými typy zahušťovadel ve stejném poměru jednotlivých složek. Zjištěné poznatky z kontaktních simulátorů byly následně ověřeny na reálných kuličkových ložiscích, kde byla pomocí kapacitní metody měřena tloušťka mazacího filmu v EHL kontaktu. Výsledky byly porovnány se současnými predikčními vztahy pro vývoj normalizované tloušťky v kuličkovém ložisku. Bylo zjištěno, že současné predikční vztahy nedokážou dobře předpovědět chování některých typů plastických maziv, což je způsobeno schopností určitých typů zahušťovadel podílet se na tvorbě mazacího filmu. Hlubší porozumění mazacím procesům plastických maziv v EHL kontaktu kuličkových ložisek umožní přesnější vývoj nových plastických maziv a zpřesnění stávajících predikčních vztahů pro normalizovanou tloušťku mazacího filmu.

# KLÍČOVÉ SLOVA

Tribologie, Kuličkové ložisko, Plastické mazivo, EHL, Zahuštovadlo, Základový olej

# CONTENT


| | | |
|---|---|---|
| **1** | **INTRODUCTION** | **9** |
| **2** | **STATE OF THE ART** | **11** |
| 2.1 | Ball bearings | 11 |
| 2.2 | Lubrication of ball bearing | 12 |
| 2.2.1 | Grease definition | 12 |
| 2.2.2 | Grease lubrication phases for ball bearings | 13 |
| 2.2.3 | EHL contact | 15 |
| 2.2.4 | Starvations | 17 |
| 2.2.5 | Lubricant Replenishment | 20 |
| 2.2.6 | Grease in EHL contact | 22 |
| 2.2.7 | Measuring film thickness in a rolling bearing | 25 |
| **3** | **ANALYSIS AND CONCLUSION OF LITERATURE REVIEW** | **29** |
| 3.1 | Effect of contact conformity on grease lubrication | 29 |
| 3.2 | Differences in thickener behaviour: Ball-on-disc vs. Ball bearing contacts | 30 |
| 3.3 | Transferability of the result from optical tribometers to real ball bearings | 31 |
| **4** | **AIMS OF THE THESIS** | **33** |
| 4.1 | Scientific questions and hypotheses | 33 |
| 4.2 | Thesis layout | 34 |
| **5** | **MATERIALS AND METHODS** | **36** |
| 5.1 | Laboratory experimental devices | 37 |
| 5.1.1 | Ball-on-disc optical tribometer (BoD) | 37 |
| 5.1.2 | Ball-on-Ring optical tribometer (BoR) | 38 |
| 5.1.3 | Real ball bearing experiments | 39 |
| 5.1.4 | Apparent viscosity | 39 |
| 5.2 | Experimental methods | 40 |
| 5.2.1 | Colorimetric interferometry | 40 |
| 5.2.2 | Fluorescent microscopy | 41 |
| 5.2.3 | Capacitance method | 43 |
| 5.3 | Experiment design and methodology | 45 |
| 5.3.1 | Paper A | 45 |
| 5.3.2 | Paper B | 46 |
| 5.3.3 | Paper C | 48 |

5.3.4 Paper D 50

**6 RESULTS AND DISCUSSION 52**

**7 CONCLUSIONS 113**

7.1 Recommendations for future research 114

**8 LIST OF PUBLICATIONS & OUTCOMES 116**

8.1 Publications related to the topic of this thesis 116

**9 LITERATURE 117**

**LIST OF FIGURES 126**

**LIST OF TABLES 128**

# 1 INTRODUCTION

Improving and streamlining machines and their components is necessary due to the demands of the current market. The main focus is on increasing efficiency, reliability, and reducing environmental impact while also reducing costs. A large part of the world's energy is used to overcome passive energy losses, which often arise from mechanical energy transformations and are accompanied by frictional losses, wear, and fatigue of contact surfaces. One of the most common machine components is the ball bearing, which can be found in almost all machines with rotary motion. The number of bearings currently in use worldwide is estimated to be in the range of tens of billions. Even a slight improvement in efficiency or an increase in bearing life has a huge impact on the machinery industry and the environment in general.

Lubrication is essential for the proper functioning of bearings, and in 90% of cases, it is provided by greases. These lubricants are composed of a base oil, thickener, and additives and form a so-called elastohydrodynamic lubrication (EHL) between the metal rolling elements. This type of liquid film lubrication is typical for non-conformally curved surfaces in relative motion, where the surfaces are separated by a continuous lubricating film. This mode is characterized by small contact areas and high contact pressures, with the film thickness usually being of the same order of magnitude as the elastic deformation of the surfaces. EHL provides the lowest friction compared to other lubrication regimes, hence the desire to maintain machine elements in this regime. If sufficient lubricant is available around the contacts, we speak of a fully flooded contact, and the lubrication film thickness is determined by the friction velocity of the surfaces, their geometry, lubricant properties, load, and ambient temperature.

However, in the case of rolling bearings lubricated with grease, there is often a situation where the contacts have to work with a limited amount of lubricant. Such a lubricated contact is referred to as starved or under-supplied with lubricant. This is a riskier situation where thinner lubrication films are formed than in a fully flooded EHL contact. In the case of thinner lubrication films, the roughness of the contact surfaces may come into contact and interact, leading to the initiation of pitting or spalling fatigue damage. Therefore, there is a general effort to thoroughly understand the lubrication mechanisms inside rolling bearings lubricated with greases to predict lubrication thickness accurately and to prevent negative phenomena in time.

Currently, the most prevalent type of grease used to lubricate rolling bearings is lithium-based grease. The transition to electric vehicles instead of internal combustion engines has resulted in an increase in the market price of lithium. Consequently, there is a rising demand for viable alternatives such as polyurea-based greases. Over recent decades, theoretical models have been developed to describe both starvation and the behaviour of greases in ball bearings. These models have primarily addressed the behaviour of the most common

lubricants, namely lithium-based ones. However, new greases exhibit different behaviours both directly in EHL contacts and across the entire bearing. Therefore, relying solely on theoretical models may not suffice or provide accurate predictions for these new types of greases.

This dissertation focuses on studying individual grease components in starved EHL contacts and demonstrates the correlation between experimental approaches used in grease lubrication studies. The findings from experiments with simplified geometries were compared with experiments conducted on real ball bearings. The greases without additives were employed for the experiments, including both lithium-based greases, the most commonly used type, and polyurea-based greases, representing a new trend in grease lubrication.

A more thorough understanding of the behaviour of individual grease components in EHL contact will facilitate improved grease formulation and more precise predictions of radial ball bearing behaviour. Ultimately, this could result in cost savings through the adoption of more economical grease alternatives and the prevention of potential failures in these mechanical components. Ball bearings are among the most widely used engineering components in the world and an essential part of almost all machinery. Even a slight improvement in durability or reliability can have a significant impact on the industry as a whole.

# 2 STATE OF THE ART

## 2.1 Ball bearings

Fig. 1. shows a single deep groove radial ball bearing, which is the most common type of rolling bearing and one of the most widely used machine parts in the world. [1]. These bearings play a key role in a wide range of applications, from automotive systems, marine vessels and spacecraft to space satellites. According to its name, it is a rolling bearing in which the rolling of individual components is accompanied by low frictional losses. In approximately 90% of cases, lubrication is provided by greases, which are essential for maintaining the operational efficiency and durability of the bearings [2].

Fig. 1 A single deep-groove radial ball bearing.

Ball rolling bearings consist of an outer ring, an inner ring, rolling elements, and a cage or seal. Grooves are formed in both the outer and inner rings, with a radius of curvature between 51.5% and 53% of the ball diameter[3]. Due to the resulting conformability, a deep groove ball bearing has a relatively high load-carrying capacity when accurately manufactured from quality steel and properly lubricated. Bearings are primarily used to carry radial loads, but they also perform well with combined radial and axial loads or axial loads only. The deep groove ball bearing can easily be fitted with seals or covers. These components serve to retain the lubricant within the bearing and protect it from contaminants.

Ball bearings are typically made from steels that are well-hardened, at least on the surface. AISI 52100 steel, which is moderately rich in chromium, is commonly used in the manufacture of ball bearings. This steel can be hardened continuously throughout its surface to a hardness of 61-65 Rockwell C. However, for miniature ball bearings, stainless steel components such as AISI 440C are often preferred [3]. Cage materials are usually softer compared to ball and ring materials. They must also have a good strength-to-weight ratio;

therefore, materials such as mild steel, bronze, polyamide (nylon), and polytetrafluoroethylene (Teflon or PTFE) are used for cages.

## 2.2 Lubrication of ball bearing

### 2.2.1 Grease definition

A grease is defined as "a solid to semi-liquid product or dispersion of a thickener in a base oil, possibly with the addition of other components to improve its properties" [2]. The retention of the base oil in the thickener matrix is made possible by a combination of Van der Waals and capillary forces. Molecular interactions between thickeners include dipole-dipole interactions, such as hydrogen bonding [4] as well as ionic and Van der Waals forces [5]. The effectiveness of these forces depends on how the thickeners interact. These fibres exhibit lengths ranging from approximately 1 to 100 microns, with a length to diameter ratio of 10 to 100, and this ratio correlates with the consistency of the grease at a given thickener concentration [6] .The grease usually exhibits a semi-plastic behaviour that prevents leakage from the bearings.

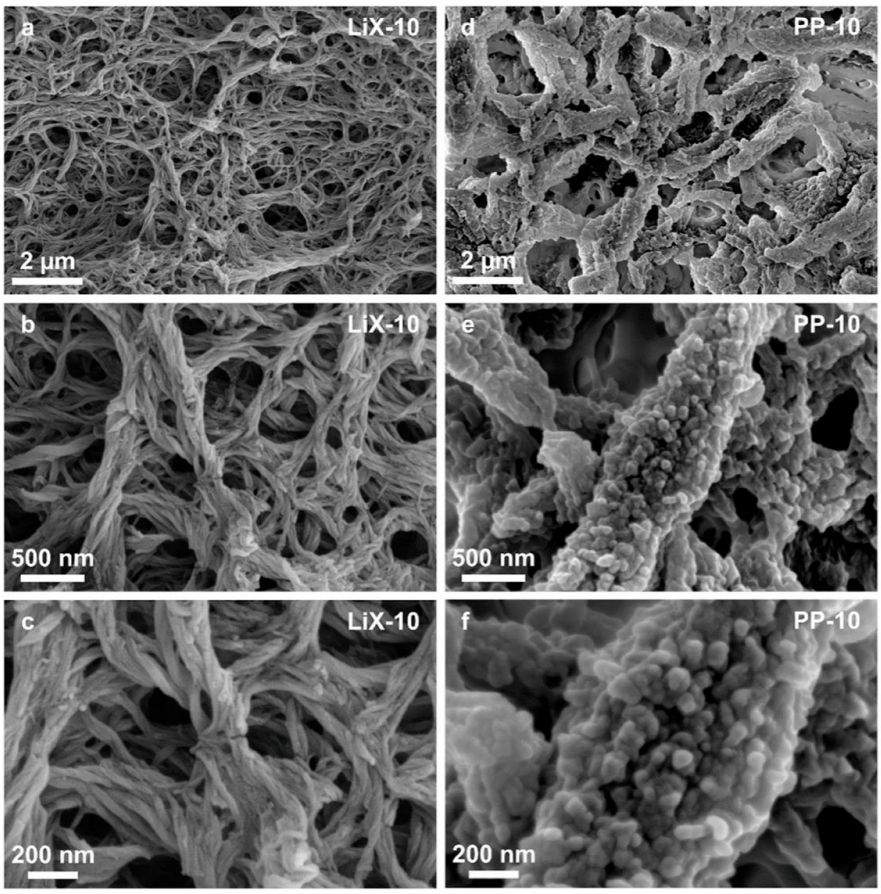


Fig. 2 Example of thickener microstructures (Lithium complex x Polypropylene thickener)[7]

Grease typically contains 80-90% base oil, with the remainder consisting of thickener and additives. As a result, grease exhibits viscoelastic behaviour, displaying viscous properties in shear rates similar to the rheology of the base oil [8]. At zero or very low shear rates, it shows plastic or solid-like behaviour. This solid-like behaviour or resistance to flow is usually characterized by consistency or penetration, measured with a cone penetrometer (ISO 2137, ASTM D217), and expressed as an NLGI consistency number. In bearings, grease is subjected to significant mechanical stress, affecting its rheological properties, especially at shear rates. The loss of consistency is quantified by comparing the mechanical stability before and after working the grease.

### 2.2.2 Grease lubrication phases for ball bearings

Grease lubrication can be divided into two basic phases Fig. 3. The first phase occurs in the initial hours of bearing operation and is called the churning phase [9]. Once the bearing is filled with grease and rotation begins, the grease starts to flow inside the bearing. The recommended amount of grease should be around 30% of the free volume of the bearing. Some of the grease flows within the bearing and tends to stick (form reservoirs), for example, under the cage or in the cage pockets. Frictional torque tends to be higher due to the relatively high viscosity of the grease, which causes the bearing temperature to rise. This phase is influenced by the internal design of the bearing and the rheological properties of the grease. The churning phase usually takes a few hours or tens of hours and depending on the percentage of fill, speed, and rheological properties of the grease. During most of this phase, the contacts are fully flooded with grease, which consists of both thickener material and oil. During this phase, the grease is heavily mechanically processed, and the portion of the grease that participates in the flow longer is significantly degraded.

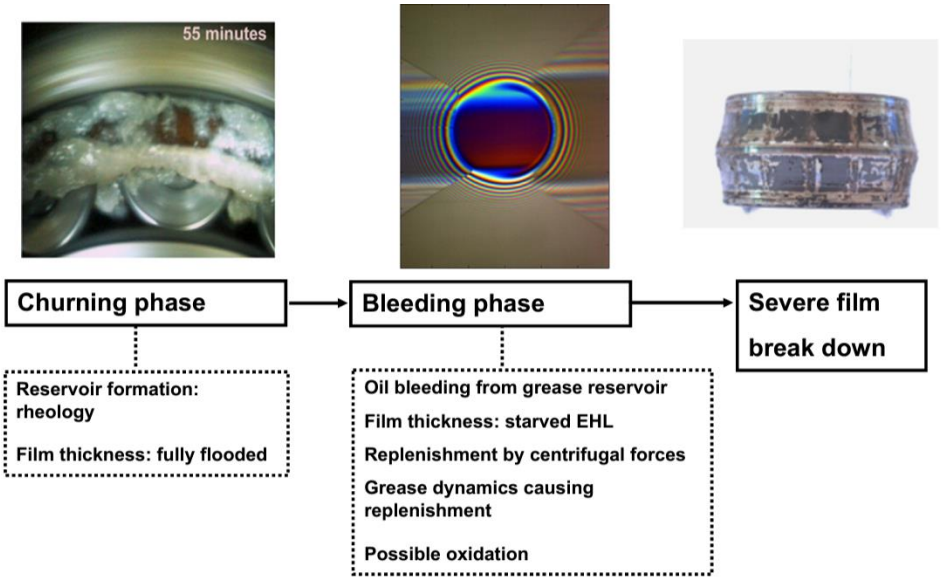


Fig. 3 The phases in the grease lubrication process [9]

After the formation of the grease reservoir, a small amount of thickener remains on the raceways, which is mechanically processed by contact passes. This is followed by a bleeding phase which persists for most of the bearing life. Compared to the churning phase, the frictional losses in the bearing during this phase are significantly lower because there is no further grease transfer within the bearing [10]. The bleeding phase is controlled by a property of the grease called the bleeding rate, i.e. the rate at which the base oil is released. This oil is released from the grease reservoirs and is the main source of lubrication for the contacts. During this phase, the bearings operate in starvation mode because the reservoirs have a limited amount of lubricant available and the film thickness may not increase with increasing speed.

Compared to the churning phase, there is less mechanical stress on the grease. Lubricants can be divided into two categories based on the length of the churning phase: "poor type" and "good/peak type" [11]. The main difference lies in the length of time the grease flows through the bearing before it settles and the bleeding phase begins

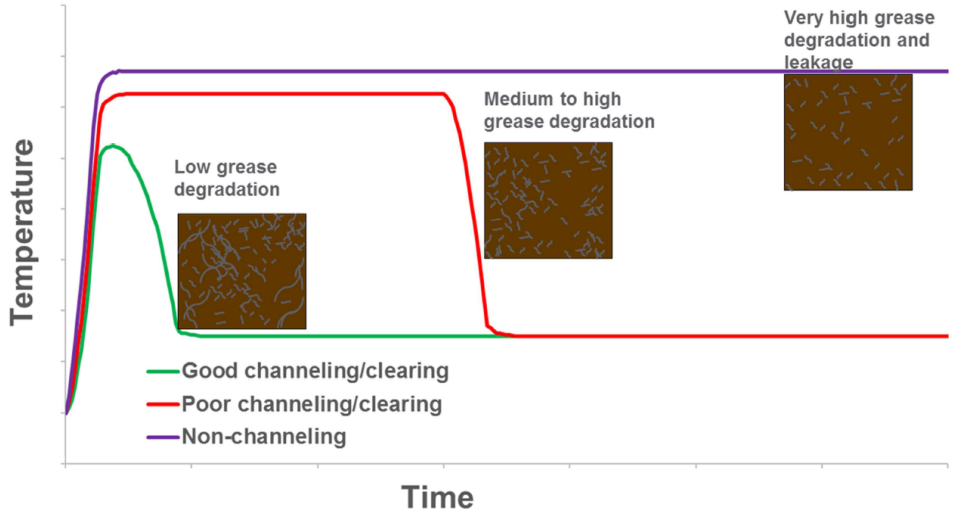


Fig. 4.

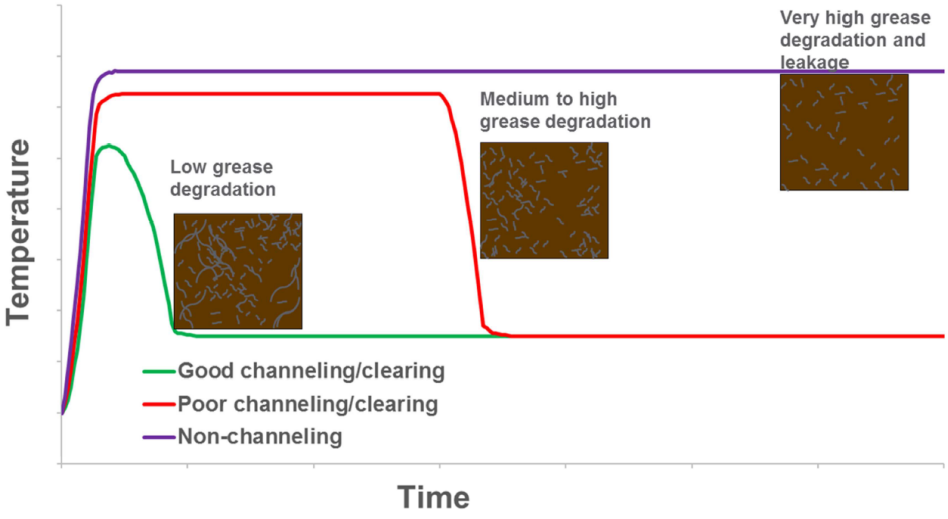


Fig. 4 Schematic representation of different types of grease behaviour during the churning phase [12]

During the bleeding phase, the so-called supply and loss mechanism described by Wikström and Jacobsson [13] occurs, where the resulting film thickness is determined by the balance of oil supply and loss in contact. Oil is added to the contact primarily by centrifugal and capillary forces. The contact pressure between the rings and rolling elements pushes the lubricant out, with some of the lubricant being used to lubricate other contacts. Lubricant loss is due to evaporation and oxidation and polymerisation can occur in the oil, affecting its properties. Centrifugal forces can also cause lubricant leakage.

If the lubrication film is thin, wear of the surfaces can occur. This process is accompanied by an increase in bearing temperature, which affects the viscosity of the lubricating oil in the lubricant. This reduction in viscosity allows the release of fresh base oil, which is forced into the contact surface by replenishment mechanisms [14]. Repeated fluctuations in temperature and lubricant thickness occur during bearing operation. Prolonged increases in temperature can damage the bearing and cause the lubricant to age more rapidly. At the end of the bearing life, the ability to sufficiently release fresh base oil is lost, leading to bearing seizure.

### 2.2.3 EHL contact

Contact situation in a rolling bearing is a frequently presented example of an Elastohydrodynamic lubrication regime, abbreviated as EHL. It involves the contact of two non-conformally curved surfaces, where rolling elements roll along the bearing rings. The surface velocity of these rolling elements and the bearing rings is (almost) equal, which means that the lubricant in the vicinity of the contact has the same velocity[15]. The lubricant is forced into the gap between the two surfaces, forming a hydrodynamic film Fig. 5. However, the contact load induces a back pressure that reduces the flow, and the thickness of the film will be the result of the balance between these two effects. The thickness of the hydrodynamic film is determined by the geometry of the bodies, the velocity, elasticity, and contact load, as well as the rheology (viscosity) of the lubricant.

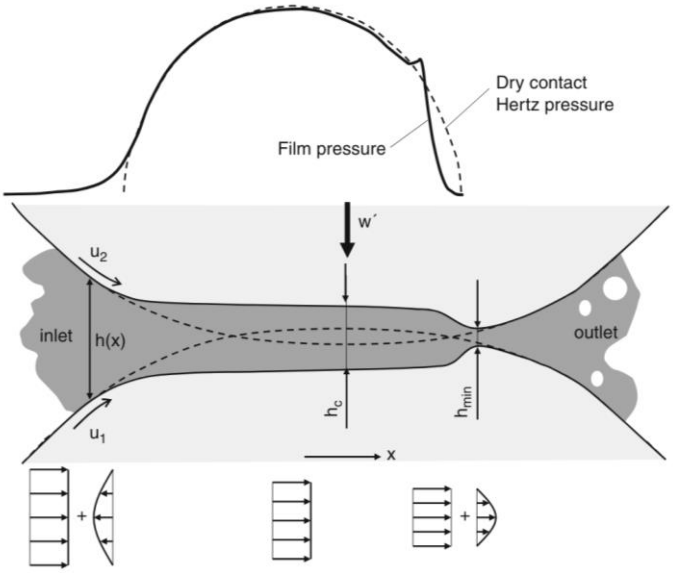


Fig. 5 Typical film thickness profile for an EHL line contact[15]

Reynolds equations for hydrodynamic lubrication were used to describe the EHL lubrication regime[16]. However, when this theory was applied to non-conformal contacts such as bearings and gears, the lubrication film thicknesses obtained were too small for these machine assemblies to operate successfully. Subsequently, Meldahl in 1941 [17] included elastic deformations of the contact surfaces, yet the predicted film thicknesses remained inadequate. In 1945, an increase in lubricant viscosity due to high contact pressure was included, resulting in a successful increase in film thickness. A numerical description of the EHL problem followed in the 1960s when Dowson and Higginson [18–20] introduced equations for film thickness under linear contact. Later, Hamrock and Dowson [21–24] introduced equations for circular contact to determine the mean and minimum film thickness under fully flooded conditions, which are still used today. In 1994, Nijenbanning et al. [25] introduced a new equation for film thickness and refined its accuracy.

Fig. 5 can be used to describe the lubricant flow in the contact. The film thickness in the EHL contact is determined by the pressure rise at the contact inlet. Due to the shape of the deformed contact bodies at the inlet, the Poiseuille flow creates a significant pressure gradient[15]. Based on the Reynolds equation, the Poiseuille flow is balanced by the Couette flow, which represents the entraining flow velocity derived from the mean velocity of the contact surfaces. Load and contact materials have minimal effect on the film thickness. The volume of lubricant drawn into contact is limited, which can lead to backflow and recirculation of lubricant prior to contact. This leads to shear flow, which reduces the viscosity of the lubricant due to shear heating at the inlet, thus affecting film thickness.

### 2.2.4 Starvations

The amount of lubricant supplied to the EHL contact also affects the thickness of the lubricating film. In Fig. 2.1, the distribution of lubricating film thickness and pressure as it passes through the contact (comparison of a fully flooded contact and a starved contact). Under starvation conditions, the available area for pressure rise is limited due to lack of lubricant [26]. In this case, the contact pressure is different compared to a fully flooded contact, and there is less lubricant film formation than under fully flooded conditions[27].

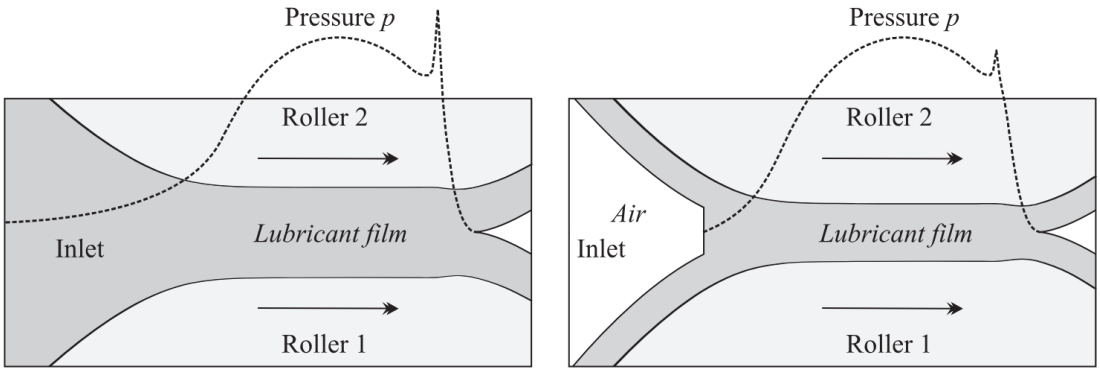


Fig. 6 Difference of lubricant distribution in fully flooded and starved contact [28]

The starvation issue was first studied by Orcutt and Cheng [29] , who observed the position of the oil entry boundary closer to contact. They were the first to establish the relationship between the meniscus and central thickness in the contact. [30] further studied the issue of starvation and proposed an empirical relationship between the starvation level and the position of the inlet boundary from the pressure region. Wolveridge et al. [31] further described the starvation of line contact. An extension of this study can be considered the work of Hamrock and Dowson [22], who developed a model in which the contact zone is divided into uniform rectangles, each considered to have uniform pressure. However, the issue of starvation was still based on the position of the meniscus.

Chevalier et al. [26,32]changed the approach by using the thickness of the lubricant entering the contact instead of its position. The starvation level is then defined by the ratio of the lubricant thickness at the contact entry to the central thickness at fully flooded contact. Damiens et al. [33] developed a model using the parameter γ to determine lubricant loss due to lateral flow. Fig. 7 shows the dependence of the central thickness in contact as a function of the amount of lubricant input. Two asymptotes are presented: the first, $H_{oil}/H_{cff}$, represents the ratio between the amount of lubricant at the inlet and the central film thickness of a given contact under fully flooded conditions. The second asymptote, $H_c/H_{cff}$, represents the actual thickness in contact under starvation. From the values, it can be deduced that significant starvation occurs when the amount of lubricant before contact is approximately twice the current film thickness in contact. The $H_c/H_{cff}$ asymptote was further used to determine the

breakdown of the lubricant film on the track. An analytical formula was presented that equated $H_c/H_{cff}$ with the parameter R, referred to as the reduction of the central lubricating film thickness.

The second part of this work examines the impact of repeated lubricant passage through the contact area and its effect on the degradation of the lubricating film. Using this model, the meniscus position and central thickness reduction can be calculated based on the lubricant thickness at the contact inlet. Moreover, this approach effectively describes varying levels of starvation[34,35].

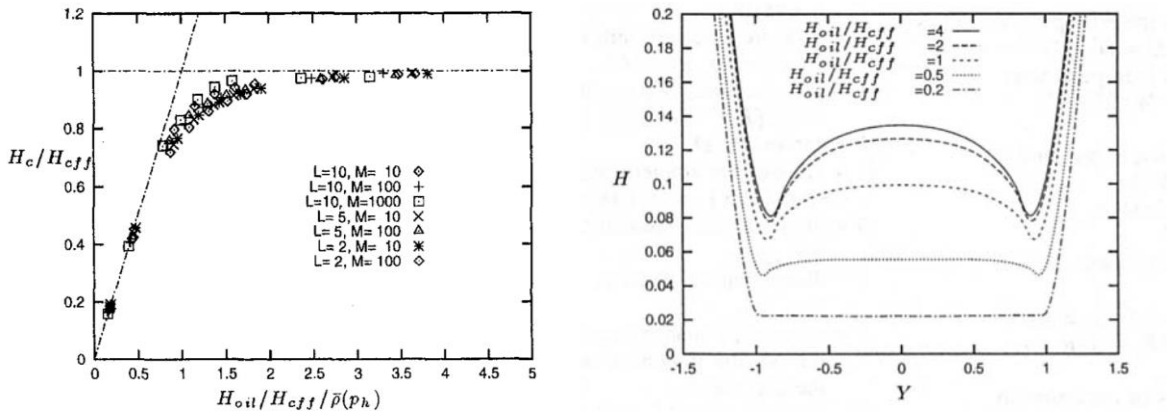


Fig. 7 Dependence of the central film thickness in contact on the amount of lubricant before contact and

Another significant contribution is the definition of the lubricating film thickness reduction due to the lateral flow of lubricant from the contact area Fig. 8 . With each additional lubricant passage, the film thickness decreases because of this phenomenon. Previous studies focusing on line contacts did not consider this effect, as lateral flow is typically ignored in such cases. However, these studies overlooked the mechanisms of lubricant re-injection into the contact. Consequently, in this model, a high number of lubricant passes lead to film failure, where the film thickness approaches zero—an outcome rarely observed in experimental settings.

$$R(n) = \frac{1}{\sqrt[\gamma]{\frac{1}{r_0^{\gamma}} + n}}, \lim_{n\to\infty} R(n) = n^{\frac{-1}{\gamma}}$$

- R - reduction of central lubrication film thickness (Hc/Hcff)
- R0 - relative lubricating film thickness Hoil / Hcff / $\rho$
- n - number of contact passes
- $\gamma$ - resistance to lateral flow
- $\rho$ - dimensionless density

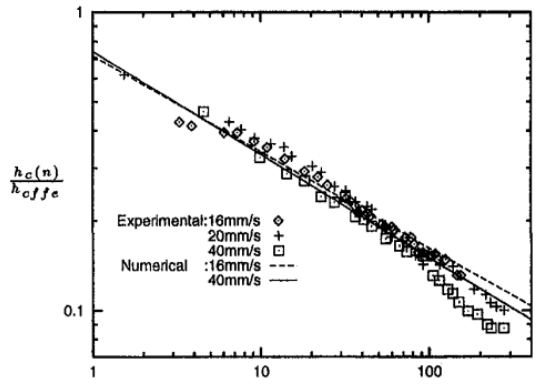


Fig. 8 Decrease in film thickness due to increase in number of contact passes

Cann et al. [36] further defined the state of transition where there is a change from the fully flooded regime to the starvation regime (degree of starvation-SD). The SD parameter offers a description of the starvation level using a single number and is defined by five parameters. Starvation is positively influenced by the amount of lubricant and surface tension. As speed, viscosity and contact size increase, starvation is more easily achieved. The model considers local replenishment processes and does not consider lateral lubricant discharge. The transition occurs at an SD parameter value of 1.5 Fig. 9. The relationship between SD parameter and film thickness was determined as follows: SD < 1.5 - $h_c / h_{cff} = 1$ and for SD > $h_c / h_{cff} = (1.5 / SD)^{1.67}$.

$$SD = \frac{\eta_0 * u * a}{h_{oil\infty} * \sigma_s}$$

- SD - Starvation degree
- $\eta_0$ - Dynamic viscosity of the lubricant
- $u$ - Speed
- $a$ - width of the rolling path
- $\sigma_s$- surface tension
- $h_{oil\infty}$- amount of lubricant near the contact

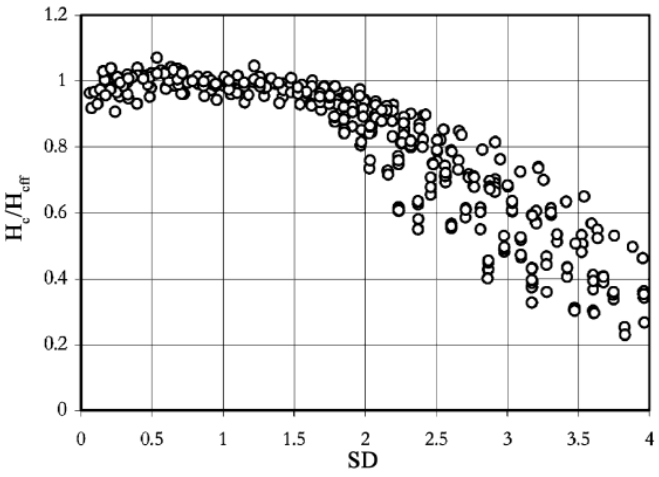


Fig. 9 Dependence of starvation level on SD parameter

Van Zoelen et al. [37] presented a model that can simulate the lubricant film drop for a complete ball and spherical roller bearing. He showed the effect of centrifugal shear stress on the oil film and its ability to supply the contacts. Venner et al., in another work [38], extended the previous models to include greases Fig. 10, which have complex rheologies and consist of multiple components with different properties in contrast to liquid lubricants. Additionally, the model addresses lubricant layer migration caused by centrifugal forces. The decay time of the lubrication layer depends on the bearing speed; higher speeds result in longer decay times. The assumed decay time for a spherical bearing is longer than that for a ball bearing. Radial load has minimal effect on the bearing. The model predicts that the breakdown times of the lubrication layer thickness are much shorter than the typical operating times observed in practice. The results indicate that a bearing cannot maintain a sufficient base oil layer on the raceway without significant replenishment.

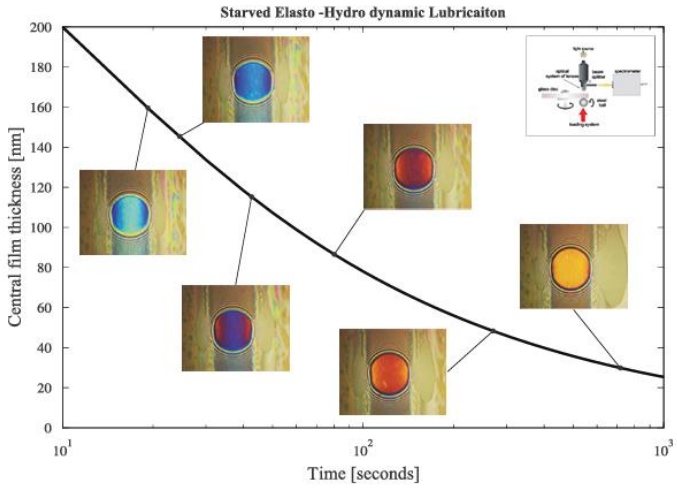


Fig. 10 Central film thickness decay in a starved circular EHL contact as a function of time.

### 2.2.5 Lubricant Replenishment

The starvation of EHL contact is counteracted by several mechanisms. Chiu [39] was one of the first to study the phenomenon of lubricant replenishment into the rolling path. After passing through the contact, the lubricant tends to reform a uniform layer, with surface tension playing a major role. Pemberton and Cameron [40] conducted a study on

replenishment, visualizing the lubricant around the contact Fig. 11. They observed that the lubricant tends to form two lateral reservoirs, which act as lubricant sources for the contact.

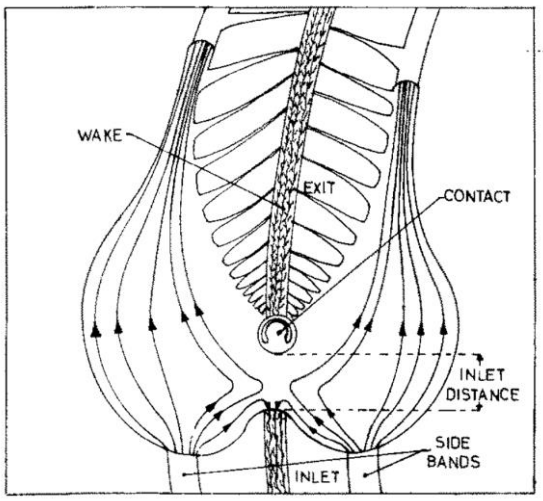


Fig. 11 Lubricant flow pattern around the EHL contact

In a previous paper, she mentioned surface tension as the main force acting in the replenishment mechanism. However, surface tension does not explain the region of extreme starvation (parched lubrication)[41], where there is not a complete failure of contact, but rather a stabilization at around 10-20 nm. Guangteng and Spikes [42,43] tried to enhance Chiu's [39] existing model by incorporating Van der Waals forces. Jacod et al. [44] published a continuation of the study on the influence of Van der Waals forces. From their models, it can be concluded that without a lubricant replenishment mechanism in contact, failure will inevitably occur after some time.

The effect of lubricant replenishment after exiting contact and returning to the rolling path Gershuni was also studied numerically by Nogi [45][46], who used the Coyne-Elrod theory to determine the position of the inlet. Previous lubricant replenishment models did not consider centrifugal or gravitational forces. Gershuni [47] added the effect of centrifugal forces to the model and emphasized its importance for real applications. For bearings operating at higher speeds, the effect of centrifugal forces is more pronounced. The authors noted that the times between rolling element passes are significantly shorter than those measured, yet they may still have practical applications. For instance, this could apply to long-term lubricant migration in bearings and its accumulation in certain areas. The behaviour of the free lubricant layer on the surfaces of tapered roller and spherical roller bearings was investigated by Van Zoelen [48]. His main aim was to complement previous models by analyzing the movement of the free lubricant layer on the bearing contact surfaces. This is because their geometry allows the movement of the lubricant over the free surface due to centrifugal forces. Lubricant replenishment around the EHL contact was also studied by Fischer et al. [49] using CFD simulations. They found that starvation depends on the capillary number, which is a function of viscosity and surface tension. Based on this,

they determined the transition from fully flooded conditions to starved lubrication. The resulting meniscus distance was strongly influenced by the amount of lubricant and the wetting of the surfaces. It was shown that a larger contact angle between the lubricant and the surface helps to increase the distance of the meniscus from the contact. When comparing different amounts of lubricant and contact angles, it was found that the meniscus distance decreases similarly with decreasing amounts of lubricant. The lubricant contact angle significantly impacts the shape of the lateral reservoirs, which are directly responsible for meniscus formation. Increasing the amount of available lubricant has a positive effect on meniscus formation, but this is limited by the formation of the lateral reservoirs. Once a certain amount of lubricant is reached, the prolonged state of the distribution no longer exhibits the characteristic "butterfly shape".

After the lubricant leaves contact, it tends to adhere to both surfaces. This issue was addressed by Chong [50], Bruyer [51], who also considered the effect of the slip ratio. In this study, the effect of the SRR (slip ratio) on the lubricant partitioning between two surfaces leaving the contact area was investigated. The results of this partitioning were presented in the numerical model section. For extreme SRR values of -2 and 2, one surface remains static, meaning that all the lubricant passing through the contact is carried away by the other, moving surface. Based on the numerical solution, the authors proposed an analytical relationship for calculating the lubricant partition ratio between the surfaces, demonstrating that the partition ratio depends solely on the slip ratio between the surfaces.

### 2.2.6 Grease in EHL contact

The behaviour of grease in Elastohydrodynamic lubrication (EHL) contacts has been extensively studied using an optical tribometer in a ball-on-disc configuration. One of the pioneering researchers in this field was Åström [52,53] , who provided early descriptions of grease behaviour. The formation of film thickness in grease differs from that of oil, with less pronounced starvation processes, as demonstrated by Cann [54][55]. However, similar phenomena occur in both grease and base oil contexts. The presence of a thickener in grease notably increases the film thickness, a topic that has been significantly explored in the literature [56–59].

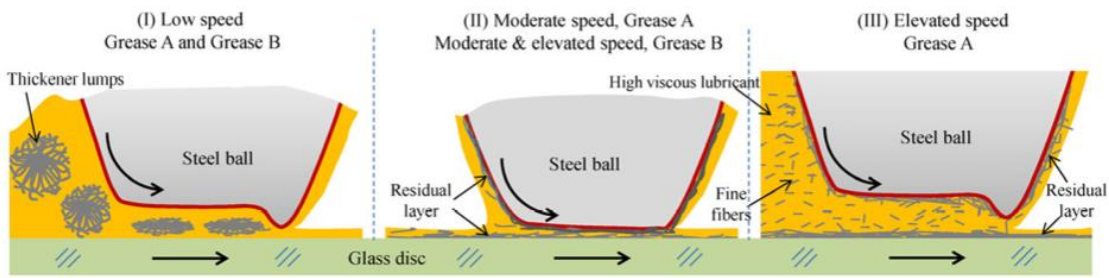


Fig. 12 Different lubrication states in different conditions [59]

Another way to study grease behaviour was through modelling. Studies often use the assumption that greases behave like Bingham liquids. This approach has been used by authors such as Greenwood and Kauzlarich [60] or Dong and Qian [61]. These models show the influence of the rheological properties of greases, which are directly affected by manufacturing processes such as preparation temperatures and post-production homogenization. Further influence is seen when the chemical composition of the grease changes. However, the models do not account for changes in these rheological properties during bearing operation, such as during the passage through the EHL contact when the thickener fibres break under pressure or during the bearing's churning phase when shear degradation occurs. Other uncertainties arise due to elevated temperatures that initiate chemical oxidation and the loss of base oil from the structure during the bleeding phase.

However, the change in rheological properties was well studied using a ball-on-disc tribometer [62]. For example, Hurley and Cann [63–65] tested thermally degraded greases against fresh greases and demonstrated that thermal degradation directly affects the ability to prevent starvation of EHL contacts. Additionally, the entire process of thermal degradation is accelerated by oxidants such as iron oxide, copper, or bronze. The oxidation process directly affects the ability to release new base oil from the thickener structure.

Cann and Lugt conducted experiments that showed mechanically degraded grease has different properties than fresh grease [66–68]. Shear stress causes the thickener fibres to break down, resulting in a film thickness that closely resembles that of the base oil. However, if thermal degradation also occurs, the expelled base oil has a higher viscosity, leading to the formation of a thicker lubricating film Fig. 13.

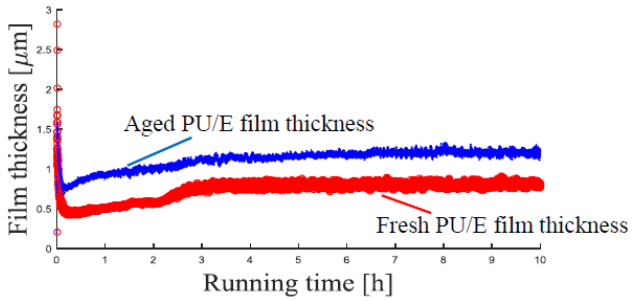


Fig. 13 Film thickness profiles for fresh and aged PU/E [67]

In the bearing, thermal and mechanical ageing occur simultaneously, with the film thickness also affected by the evaporation of base oil from the thickener structure. Fig. 14 schematically illustrates the evolution of film thickness in such a bearing.

Initially, the grease layer thickness equals that of fully flooded oil, but starvation occurs almost immediately, potentially leading to film collapse if the contacts are not replenished with oil[69–71]. The minimum film thickness occurs at the crossover point, where sufficient oil discharge halts further thinning. Thereafter, the film thickness increases until a balance is reached between the supply and loss of lubricant at the contact. After a much longer period,

the film thickness decreases again due to leakage, oxidation, evaporation, and other factors. The dominant loss mechanism will depend on the operating conditions; for example, oxidation will prevail at high temperatures.

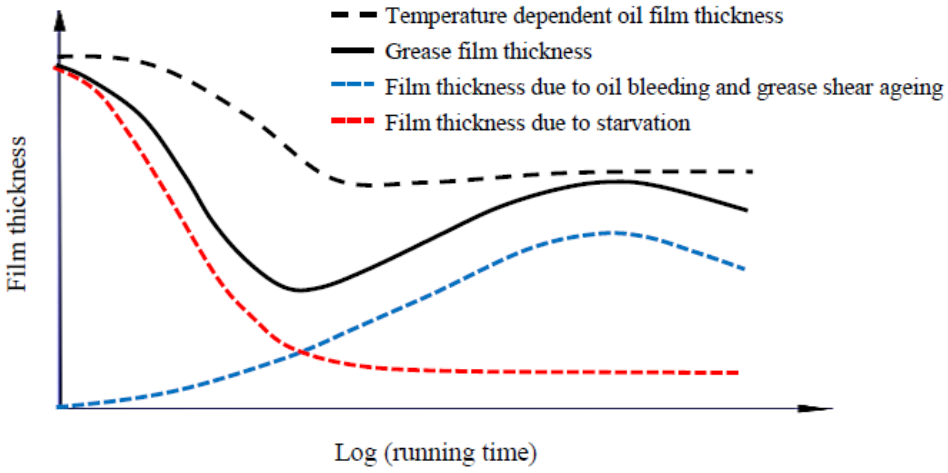


Fig. 14 Grease film thickness variation inside a rolling bearing [67]

The behaviour of grease in EHL contact is greatly influenced by the chemical nature and thickener, as well as by the operating conditions[72]. For example, Kaneta [73] highlights the behaviour of polyurea grease in both fully flooded and starved conditions. In these types of greases, the thickness is strongly influenced by the thickener, and a layer of thickener forms on the contact surfaces. The influence of operating parameters such as rolling speed or temperature was investigated by Kanazawa et al. [74,75], who related the behaviour of the thickener to the coefficient of friction. It was found that polyurea greases exhibit a higher ability to form a thickener layer at low speeds when the thickness of the lubricating film is approximately the same as the diameter of the thickener fibres. The effect of velocity was further investigated by Kochi et al. [76], who showed an increase in thickener concentration in the low-velocity region. Kochi demonstrated that the thickness of the lubrication layer formed by grease varies with speed Fig. 15. At high speeds, the grease forms an EHL layer with a thickness slightly greater than predicted by the base oil formula. As the speed decreases, the thickness deviates, reaching a minimum before significantly increasing at low speeds. This increase in film thickness at low speeds occurs because the lubricant splits into a low-viscosity phase (predominantly base oil) and a high-viscosity phase (thickener) at the EHL contact. The higher concentration of thickener at low speeds results in increased viscosity, thereby producing a thicker film in the contact. As the speed increases, the high-viscosity phase loses its non-Newtonian behaviour, reducing the tendency for the low-viscosity phase to drain. Consequently, the thickener concentration and film thickness increase diminish at high speeds.

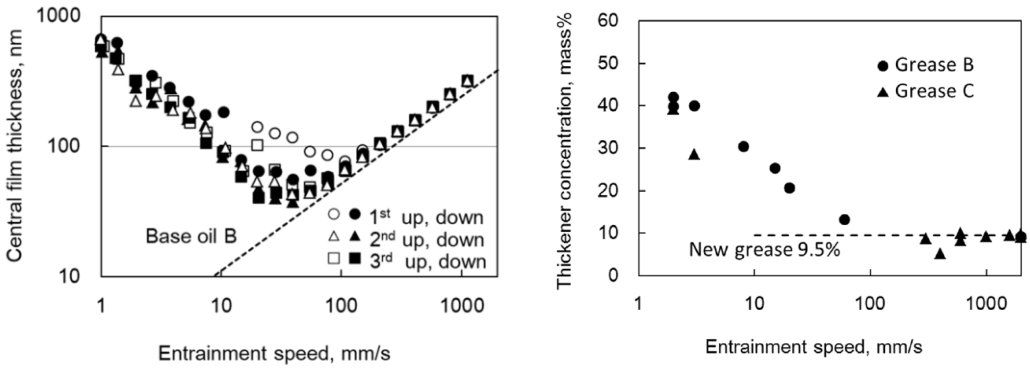


Fig. 15 Effect of speed on film thickness and thickener concentration

FT-IR (Fourier Transform Infrared Spectroscopy) is used for the chemical analysis of the thickener on the track, as demonstrated by Cann et al. [77][78][79][80] Following friction tests using the Mini-Traction Machine (MTM), IR analysis was performed on the films formed in the rolling paths between the plate and the ball. Lubricants based on lithium complex and calcium sulfonate were tested. The grease formed a robust lubricating film at low speed, reducing friction in contact. This film, associated with thickeners, formed a solid layer with a thickness of 40-100 nm (Fig. 24). IR spectra indicate that the film in the trace contains a significantly larger amount of thickener than the original grease sample.

### 2.2.7 Measuring film thickness in a rolling bearing

Measurements with real ball bearings are used to verify the observed principles of grease behaviour in contacts made on simplified tribometers. The most widely used measurements are of bearing temperature and frictional resistance. However, another important quantity is the electrical capacitance, which arises due to the lubricating film in the EHL contacts. When a voltage is applied to the bearing, with the circuit leading from the outer ring of the bearing, through the rolling element, to the inner ring, a parallel plate capacitor is formed due to elastic deformations between the balls, rings, and the lubricating film. The lubricating film between the contacts of the ball rings acts as a dielectric whose thickness directly determines the contact capacitance. This method was first used in 1979 by Wilson [81] Dyson, and Wilson [82]. Due to the real-time measurement of film thickness in the actual bearing, the capacitance method is considered one of the most useful methods. The method has been refined and extended over the years with parameters such as external capacitance. Barz et al. [83] used a correction factor to compensate for this external capacitance and thus measured the lubricating film thickness in a ball bearing. Jablonka et al. [84–86] calculated the contribution of external capacitance for both single contacts and full bearings under fully flooded conditions for measurements only.

Baly et al. [87] showed that the film thickness in the low-speed region increases with increasing speed. However, from a certain speed, the increase in thickness stabilizes as the

operating speed continues to increase. This is due to the starvation of the contacts in the bearing. Morales-Espejel et al. [58] investigated the film thickness at low bearing speed and found that in the case of grease lubricants, the film thickness in the contacts was much greater than when using a base oil.

To describe the thickness evolution, Cen and Lugt [69,70] used the normalized thickness, which is the ratio of the measured thickness to the predicted thickness under fully flooded conditions. They showed that the evolution of the normalized thickness can be described by a power law relationship based on the viscosity, contact width, and velocity parameters $\eta bu$ Fig. 16.

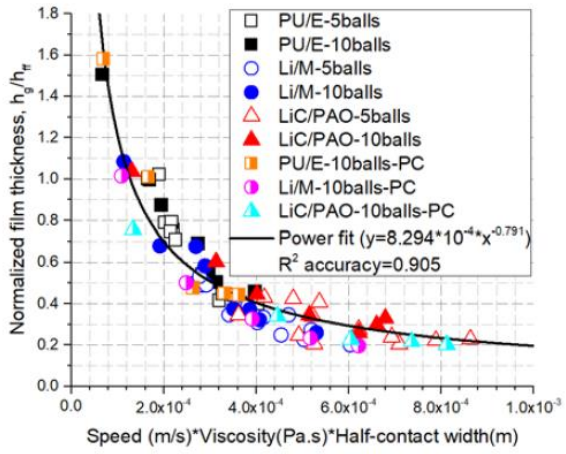


Fig. 16 Normalized film thickness in radial ball bearing

The authors observed that bearings lubricated with grease experience starvation conditions. Initially, during commissioning, the contacts are fully flooded, but the film thickness gradually decreases until a quasi-steady state is achieved, typically after 8 hours of operation. As speed increases, the film thickness stays almost constant, suggesting greater starvation at higher speeds. At these high speeds, the normalized film thickness remains stable, indicating that the film thickness might increase again, likely due to centrifugal forces that dominate the replenishment process. The impact of loading on film thickness is minimal, leading to only slight changes in geometry and compression of the lubricant in the EHL film. These measurements also reveal that the grease lubrication process is not entirely predictable. Irregular "events" occur, highlighting the chaotic nature of grease lubrication.

The development of the normalized film thickness in the bearing was not affected by the bearing stopping [88]. During the shutdown, replenishment is more efficient, but after restarting the bearing, the normalized thickness quickly returns to the expected value Fig. 17.

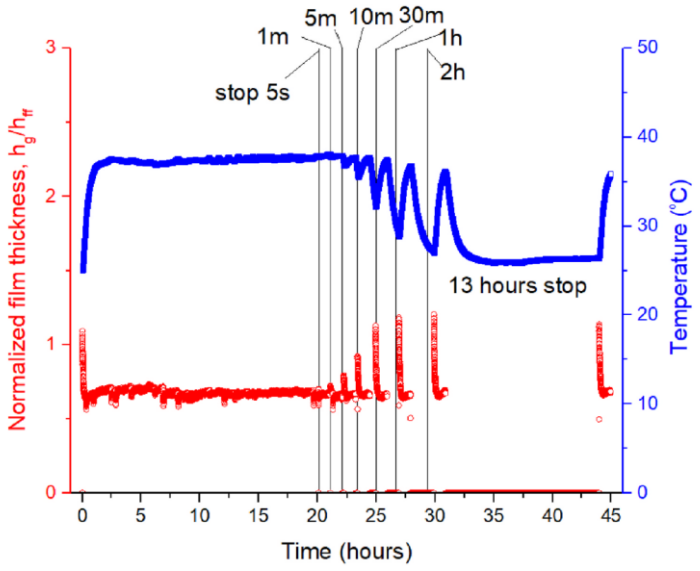


Fig. 17 Effect of stopping on the development of film thickness in the bearing

The inclusion of starvation in the thickness calculation prompted Shetty et al. [71] to consider another parameter affecting the surrounding capacitance. He then used the extended model to investigate other parameters that might influence the normalized bearing thickness. It turned out that the amount of grease dispensed does not affect the thickness evolution[89]. The influence was shown by factors that directly affect the replenishment process of the lubricant around the contact. There was an increase in film thickness when vibration was suddenly increased [90]. Another parameter investigated was the bearing size[91], where the same normalized thickness was measured on ball bearings of different sizes - 6204, 6206, and 6209 according to the parameters $\eta bu$.

As shown, the film thickness after the churning phase does not depend on the initial filling of the bearing with grease. The lubrication after this phase is provided by only a small amount of lubricant and the processes of oil replenishment around the contact and capillary action. The film thickness is affected by the evaporation of the oil film from the raceways or by leakage, occurring after a longer period of operation. Vibration tests have also shown that the film thickness increases as a function of bearing load. Due to the vibration, the ball oscillates in a curvilinear manner in the orbit, causing it to roll, which results in increased replenishment of the contacts. After reaching a certain speed, the thickness of the film in the ball bearing does not decrease with increasing speed but remains almost constant. This means that grease lubrication enables the ball bearing to function even in high-speed applications, such as bearings in electric motors in electric vehicles. The following relationship can be used to estimate the film thickness in an axially loaded deep groove ball bearing:

$$\frac{h_g}{h_{ff}} = 0.0544(\eta bu)^{-0,2945}$$

- $h_g$ - Grease film thickness in deep groove ball bearing
- $h_{ff}$ Fully flooded central film thickness in deep groove ball bearing
- $\eta$ - Base oil dynamic viscosity
- $b$ - Half contact width
- $u$ Velocity

It has also been shown that film thickness is more affected by load under starved conditions than under fully flooded conditions. At medium and high speeds, the film thickness is not dependent on the rheological properties of the grease but on the viscosity of the base oil. Under combined loading, a different film thickness was observed compared to purely axial loading. It has been shown that the volume of available grease around the contact is affected by capillary pressure, and the replenishment is a result of capillary pressure and hydraulic resistance. Thus, the length over which replenishment must take place, i.e., the width of the contact, is important. It has been shown that the determination of the film thickness in a radially loaded ball bearing can be achieved with 93% confidence and is affected by the capillary number.

# 3 ANALYSIS AND CONCLUSION OF LITERATURE REVIEW

In the literature, three main approaches are commonly used to study the behaviour of greases: experiments on a ball-on-disc tribometer, theoretical and empirical or numerical studies focusing on oils and their behaviour in EHL contacts or their vicinity, and tests on real bearings. Each of these approaches has its limitations. For example, experiments with a ball-on-disc tribometer can be affected by simplified geometry that can bias lubricant replenishment. Theoretical models primarily focus on the behaviour of the oil, and in the case of grease, the complex rheology of the grease, which changes over the course of the experiment, cannot be precisely defined. Tests with real ball bearings are powerful tools, but they do not allow direct observation of the processes in the contacts, instead monitoring the overall behaviour of the bearing.

## 3.1 Effect of contact conformity on grease lubrication

Much of the current grease research relies on ball-on-disc devices and optical observation methods[27,54,63,77,92]. However, compared to real geometry, there is a bias due to the different conformity of contacts and their shapes—circular contact versus highly elliptical contact. At medium and higher speeds, ball-on-disc devices experience rapid and severe starvation unless the lubricant is directed into the contact[27,62]. These devices are used to describe lubricant replenishment around the contact and to validate models examining parameters such as the capillary number[49]. While the device can simulate events that occur in the EHL contact, it does not effectively simulate the events around the contact that affect starvation. Nonetheless, the starvation mode is the most common mode encountered in real-world ball bearing applications[69–71].

The starvation mode is influenced by a number of parameters such as replenishment, contact ellipticity, contact width, rheological properties of the lubricant, and others[25,26,32]. For contacts with different conformity, not only does the ellipticity of the contact area vary, but the capillary effect around the contact is also affected. Studies show that the capillary effect is directly responsible for the replenishment process. This process influences the behaviour of the lubricant even after leaving the contact. It has been shown that the lubricant tends to form a uniform layer on the disc and the ball after leaving the contact[51]. However, the lubricant used to form the film thickness in the contact is present not only on the track in front of the contact but also on the sides of the contact [34,35]. Different conformity creates a differently sized gap between the element and the ring, resulting in varying amounts of lubricant around the contact. With different gap sizes between the rolling element and the ring, a different amount of lubricant always remains on the raceway, which, in combination

with the replenishment effect, can serve as a reserve of lubricant for the next contact. Another important parameter is the contact width[69,70], both on tribometers and in actual bearings. With wider contacts, the lubricant is more spread out from the centre of the raceway, and it takes longer for the lubricant to flow back to the centre of the contact[47]. Thus, different conformity combines these effects, which together result in the formation of a lubrication layer in the contact. Observations of the base oil in grease samples can be used to verify these assumptions, and the literature suggests that oil properties such as viscosity can be used to predict film thickness.

## 3.2 Differences in thickener behaviour: Ball-on-disc vs. Ball bearing contacts

The formation of the lubricating film in EHD contact for greases is influenced by many factors. In addition to the parameters relevant for base oil, the rheological properties of the grease, such as its NLGI number, thickener content, type of thickener, level of homogenization, etc., play a significant role. So far, the ball-on-disc device, which creates contact between simplified geometries, has been used for studying this phenomenon[54,55,77]. It has been shown that, under fully flooded conditions, the film thickness varies most at low speeds, where lower shear stress leads to an increased apparent viscosity of the grease and a higher concentration of thickener on the track. At higher speeds, the thickness is slightly greater than that of the base oil[69].

There is also a difference based on the type of thickener. Lithium grease exhibits a characteristic curve shape, and in long-term experiments, the thickness remains stable, with the thickener forming a layer on the track in the range of 20-40 nm [72]. In the case of polyurea [73–75] it was observed that at low speeds, the thickener can form a film that is significantly thicker (100-400 nm) due to the greater adhesion of the thickener on the track. Under starving conditions, the formation of the lubricating film is significantly influenced by the thickener. For oil, due to insufficient replenishment, the lubrication film tends to reach parched lubrication[41], i.e., the same order of magnitude as the formation of the thickener layer on the track. However, there is a noticeable difference between greases and their structure. Greases containing larger pieces of thickener can form a thicker lubricating film under these conditions[73]. In real deep groove bearing contacts, where there is greater conformity and more efficient replenishment, the amount of lubricant before contact will be significantly greater than in a ball-on-disc configuration.

Therefore, in addition to the rheological parameters of the greases, there will be more variation in operating speed, which will affect the amount of lubricant before contact. According to the literature, the replenishment of lubricant prior to contact is most dominant[47,52], with the contact retaining only a portion of the lubricant around itself.

Compared to ball-on-disc, where fresh lubricant is constantly directed into the contact, real conformity results in more stress on the thickener, hence a more limited lubricant film. Therefore, the ability to form a thickener layer in real configurations will differ from that in simplified geometries. By conducting comparative experiments with suitable greases containing different thickeners, the effect of conformity on thickener behaviour can be determined.

## 3.3 Transferability of the result from optical tribometers to real ball bearings

As mentioned, lubricant replenishment in optical tribometers is not the same as in real ball bearings due to differences in contact geometry, the effects of centrifugal forces, the influence of the cage, and other factors. We can create conditions with either fully flooded or starved lubrication. In a bearing, the situation is initially variable: during churning, the bearing is fully flooded, and then starvation occurs, which depends on lubricant rheology, load, and speed[10,11]. However, lubrication film thickness calculations typically do not consider the rheology of the grease and only account for the oil's viscosity[69,70,88]. It has been shown that greases form a layer of thickener on surfaces, increasing the film thickness at the contact points[74,75]. During the initial hours of operation under fully flooded conditions, we can expect similar trends to those observed in simplified tribometers. Most studies have focused on lithium greases, which are the most common, but polyurea greases are expected to produce different film thicknesses during the churning phase due to the form of the thickener layer on friction surfaces.

However, the film thickness values after bearing break-in are of higher priority [14,69,70,88]. After break-in, reservoirs are formed, and lubrication primarily relies on the bleached base oil. This condition is not constant, as temperature spikes can occur randomly and do not last long. These spikes can be caused by two phenomena. The first is the starvation of the contact to the point where surface roughness interactions occur, naturally raising the bearing temperature, which facilitates the release of new base oil and returns the film to a stable state and thickness. The second is the release of some grease from around the cage, aiding further lubrication [2,9]. This release can be caused by changes in bearing speed, temperature, or vibration. Some thickener is expected to remain in the lubricant around the contact after break-in, either from the churning phase or due to further loosening caused by temperature or speed changes.

In the case of greases with a lower affinity of thickener to oil, the formation of a thickener layer can continue after break-in. This effect is most dominant at slow speeds, as observed in both publications and real bearing measurements. The thickener's effect increases with apparent viscosity, which is greatest at slow speeds. At these low speeds, some agreement

in lubricating film development between optical tribometers and real ball bearings can be expected. Since thickness evolution in ball bearings is driven by $\eta bu$ parameters[71,89–91], where the thickener's role is not considered, it is anticipated that under conditions where both systems produce similar film thicknesses, the influence of the thickener and the inaccuracy of current prediction relations will be evident.

# 4 AIMS OF THE THESIS

The main objective of this doctoral thesis is to clarify the behaviour of the individual components of grease in the contact of a deep groove ball bearing. The main focus is on the investigation of the contribution of the individual components to the formation of the lubricant film. The work focuses on a combination of tests on various experimental devices using optical methods and also tests with real ball bearings. Furthermore, the difference of different experimental approaches to the study of lubrication mechanisms of greases was analysed. In order to achieve the main objective of the dissertation, the following steps were necessary:

- Development of a methodology for dyeing grease components
- Preparation of custom-made greases containing fluorescently coloured individual components.
- Development of an optical tribometer that mimics the contact geometry of a ball bearing.
- A series of experiments aimed at analysing the contribution of grease components in the lubricant film and the effect of contact geometry on grease behaviour
- Verifying experiments on real deep groove ball bearings
- Assessment of the causes leading to different behaviour of different greases in deep groove ball bearings
- Results publication and discussion

## 4.1 Scientific questions and hypotheses

***Q1.*** *What is the effect of radial ball bearing conformity on grease replenishment around the contact and the level of contact starvation?*

***H1.1*** *Greater contact conformity leads to a wider contact area, pushing the available lubricant farther away from the contact point. Consequently, it takes longer to re-flood the contact area with lubricant.*

***H1.2*** *Smaller contact conformity results in a larger gap between the ring and the ball, allowing more lubricant to stay near the contact area. This increased lubricant presence helps prevent contact starvation.*

***H1.3*** *Greater contact conformity generates a significantly stronger capillary effect, which enhances the efficiency of lubricant replenishment in the contact area.*

***Q2.*** ***How does the different replenishment of the lubricant around the contact affect the behaviour of the thickener in the contact itself?***

***H2.1*** *Certain types of thickeners can adhere to the contact surface, forming a residual thickener layer. It can be expected that the adhesion process does not occur only at a certain speed but is a gradual process influenced by the test conditions, the rheology of the grease and the amount of grease available.*

***H2.2*** *With more efficient lubricant replenishment in a realistic contact geometry, the behaviour of the thickener should be the same as in a simplified ball-on-disc contact simulator under fully flooded conditions at low speed.*

***Q3.*** ***How the type of thickener affects the lubrication film thickness in a deep groove ball bearing?***

***H3.1*** *In cases of low operating speeds on ball-on-disc equipment, it can be observed that different types of thickeners cause variations in film thickness. Under fully flooded conditions and low speeds in a ball bearing, similarities between the two systems can be observed.*

***H3.2*** *When the transit speed is exceeded, the effect of the thickener on the film thickness disappears. Therefore, even at low operating speeds, the thickener should have minimal impact on the film thickness in a deep groove ball bearing.*

## 4.2 Thesis layout

This work consists of four articles published in peer-reviewed journals. Paper A addresses the method of dyeing grease components using fluorescent dyes and subsequent observation with optical tribometers. Through fluorescence microscopy, it was possible to separately observe the base oil and thickeners in the grease samples. Paper B examines the behaviour of the base oil in grease within ball bearing contacts. The behaviour of the base oil in grease was compared to the base oil alone at different contact conformities. The effects of actual conformity on lubricant replenishment and EHL contact starvation were compared. Paper C investigates the thickeners in grease under different kinematic and lubrication conditions. Experiments were conducted using a ball-on-disc tribometer and a ball-on-ring tribometer, representing ball bearing geometry. The study also explored the properties of selected thickeners and their effects on behaviour in EHL contacts. Paper D connects the insights gained on grease behaviour in EHL contacts from optical simulators with experiments on real ball bearings. The assumptions were verified for selected thickeners, and the results were linked to a predictive model describing the evolution of normalized thickness in an axially loaded ball bearing.

**Paper A**

D. KOSTAL, M. OKAL, J. FRYZA, I. KRUPKA, AND M. HARTL, "Novel In-Situ Observation of the Grease Constituents in Elastohydrodynamic Contacts by Fluorescence Microscopy," *Tribol.Lett.*, vol. 70, no. 4, Dec. 2022, doi: 10.1007/s11249-022-01671-7. [IF = 3.2]

(Author's contribution 35 %)

**Paper B**

M. OKAL, D. KOSTAL, P. SPERKA, I. KRUPKA, AND M. HARTL, "Effect of Contact Conformity on Grease Lubrication," Lubricants, vol. 10, no. 11, Nov. 2022, doi: 10.3390/lubricants10110289. [IF = 3.2]

(Author's contribution 65 %)

**Paper C**

M. OKAL, D. KOSTAL, K. SAKAI, I. KRUPKA, AND M. HARTL, "Thickener Behaviour in Rolling Elastohydrodynamic Lubrication Contacts," *Tribol Lett*, vol. 72, no. 3, p. 72, Sep. 2024, doi: 10.1007/s11249-024-01874-0. [IF = 3.2]

(Author's contribution 70 %)

**Paper D**

M. OKAL, D. KOSTAL, J. OSARA, P. LUGT, I. KRUPKA, AND M. HARTL, "Experimental study of the effect of thickener on the film thickness in a rolling bearing at low speeds," *Tribol.Trans.*, vol. 1-13, Dec. 2024, 10.1080/10402004.2024.2431523. [IF = 2]

(Author's contribution 65 %)

# 5 MATERIALS AND METHODS

To answer the scientific questions mentioned in the previous chapter, an experimental study was conducted on three laboratory devices. A ball-on-disc (BoD) optical tribometer and a ball-on-ring (BoR) optical tribometer were used, and verification experiments on real deep groove ball bearings were also performed. In addition, some sub-tests were performed to determine the rheological properties of the tested samples. In addition, scanning electron microscope (SEM) analysis was performed on selected samples. Colorimetric interferometry method was used to measure the film thickness in the EHL contact. Fluorescence microscopy was used to observe the individual components of the grease film. The capacitance method was used to measure the film thickness in the deep groove ball bearing. A purely experimental approach was used, which can test real grease samples prepared from the manufacturer. The experimental approach also allowed precise control in the influence of individual parameters and better ensured the repeatability of the experiments. An overview of the equipment used and its interconnection with publications is shown in Fig. 188

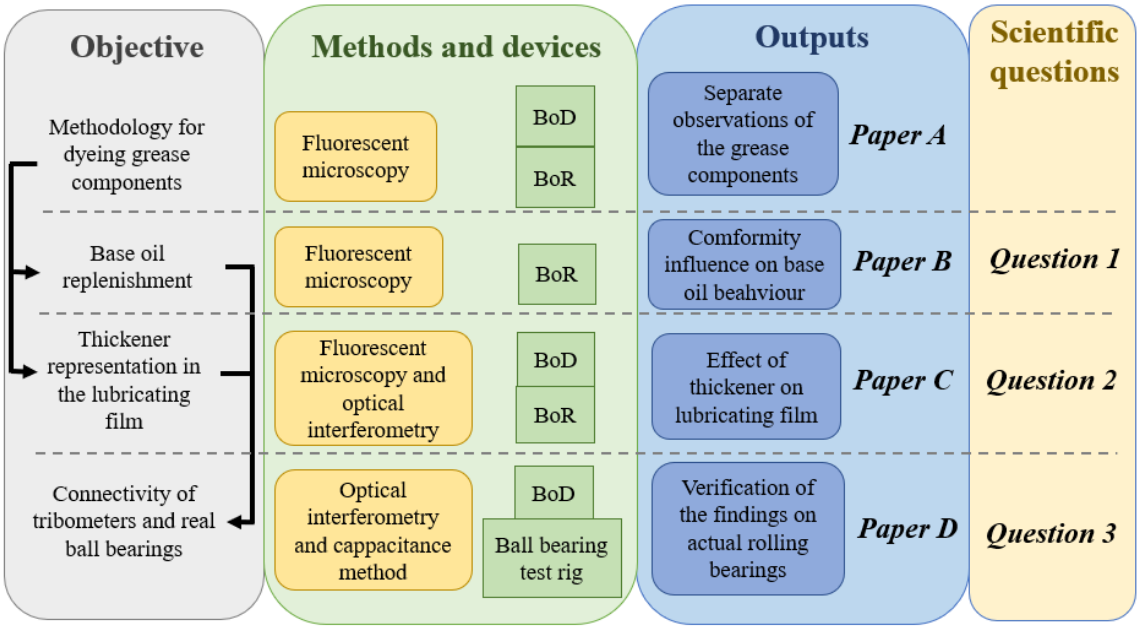


Fig. 18 Schematic representation of the link between methods and results

## 5.1 Laboratory experimental devices

### 5.1.1 Ball-on-disc optical tribometer (BoD)

Part of the experiments were performed on an in house fabricated optical tribometer of Ball-on-disc configuration. A schematic of the device is shown in Fig. 19. This is a tribological contact simulator, where the ball rolls down the underside of a glass disc, through which the contact area is observed and evaluated using optical methods. The device creates a circular EHL contact between a 25.4 mm diameter ball made of 100Cr6 bearing steel and a transparent disc made of borosilicate glass (BK7). The modulus of elasticity of the 100Cr6 bearing steel is 210 GPa and the modulus of elasticity of the BK7 borosilicate glass is 81 GPa. The surfaces of both elements are optically smooth. Both elements, the ball and the disc, are independently driven by servo motors, so different levels of slip can be created, as well as pure rolling conditions. A lever and dead weight system are used to create the load in contact. The magnitude of the load is then determined from a calibrated strain gauge built under the exciter device. The second option is to calculate the load according to the size of the contact area. The device creates fully flooded conditions due to a wiper that is pressed against the underside of the disc, directing the displaced lubricant from the contact back into the contact.

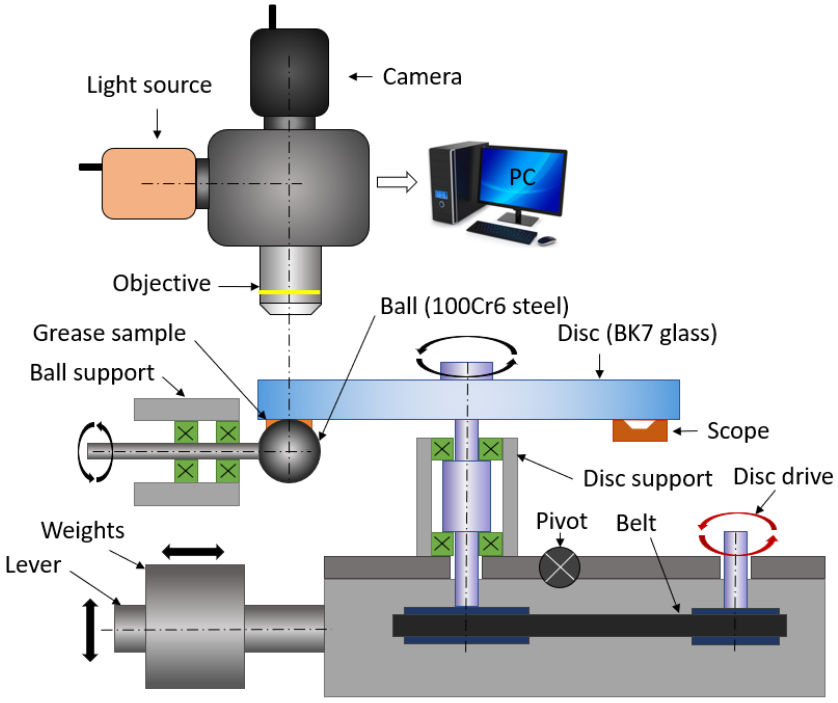


Fig. 19 Ball-on-disc optical tribometer

### 5.1.2 Ball-on-Ring optical tribometer (BoR)

The ball-on-ring configuration tribometer shown in Fig. 20 and was developed as one of the sub-objectives of this thesis. At the core of the device is a glass ring with a groove and a bearing steel ball that makes elliptical contact. The ball contained in this device can have several diameters (25.4 mm; 23.8 mm; 22.2 mm) of 100Cr6 bearing steel. The glass ring is made of BK7 borosilicate glass and has an inner groove with a radius of 13.2 mm. The total circumference of the bottom groove of the ring is 425 mm. The contact formed between these elements has a conformity of 0.52 - 0.58 and can thus mimic the contact in a 6314 deep groove ball bearing. Due to the realistic geometrical relationships, realistic lubricant replenishment is then achieved. The rolling element is pressed against the glass ring by a lever system and a dead weight. The rolling element is housed in ball bearings and shafts which generate a rectifying force directed to the centre of the ball. The device allows the experiment to be performed under pure rolling conditions. The entire ball support is mounted on a linear guide that allows the ball to self-centre at the top of the groove.

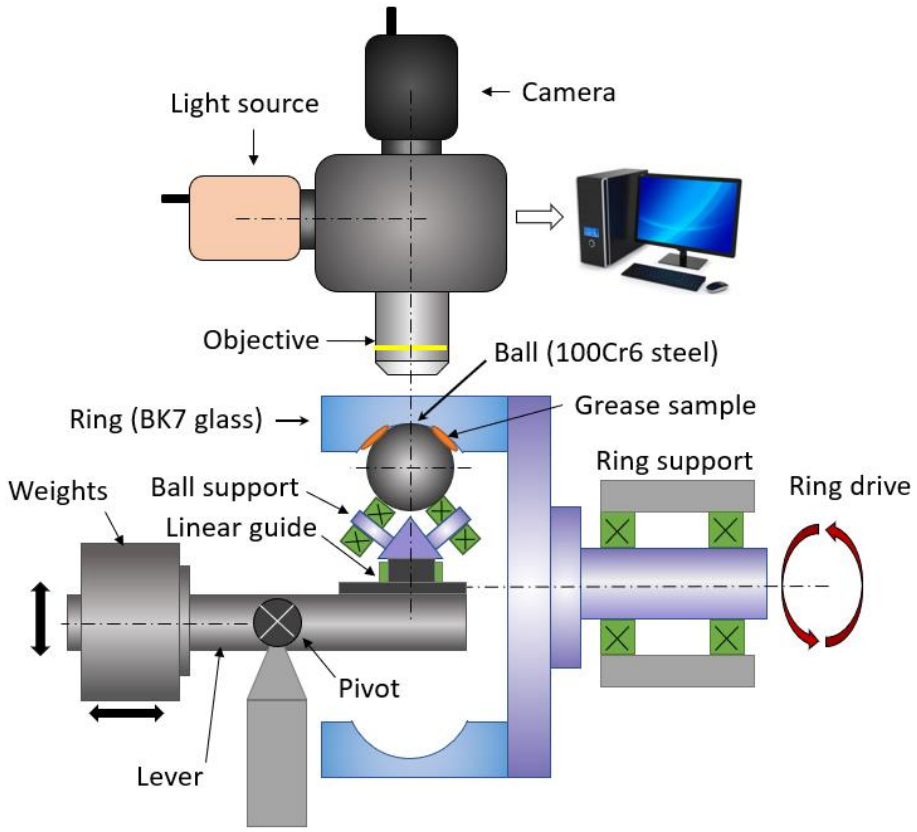


Fig. 20 Ball-on-ring optical tribometer

### 5.1.3 Real ball bearing experiments

Another device used in this study was a test rig for measuring lubricating film thickness by the capacitance method. The equipment is identical to that described in the publication [69]. The schematic of the tested bearing is shown in Fig. 21. The device allows experiments to be performed on a 6209 deep groove ball bearing. The outer ring of the bearing is insulated by a polymer bearing house and the inner ring of the bearing is driven by an electric motor. The bearing is evenly axially loaded by a pneumatic system and the resulting force is measured by a load cell. A mercury contact is used to make electrical contact with the bearing, which rotates the bearing inner ring. The non-moving outer ring of the bearing is connected to the "Lubcheck Mk3" instrument. To minimize the effect of inductance of the connecting wires, a compensation box was connected between the rings and the Lubcheck apparatus. The bearing capacitance is then measured, which the Lubcheck converts to an output voltage that is recorded in real time. The recorded voltage can be taken as a measure of the average film thickness between the inner and outer rings. The apparent viscosity of the greases was investigated using a rheometer.

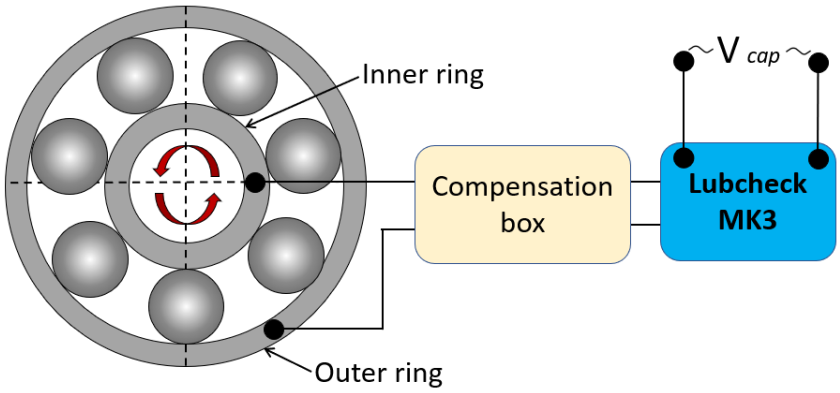


Fig. 21 Scheme of the ball bearing test rig

### 5.1.4 Apparent viscosity

The apparent viscosity of the greases was investigated using an Anton-Paar MCR 101 rheometer. The rheometer operated in a plate/plate configuration with a constant measurement gap height of 1 mm. A schematic of the rheometer is shown in Fig. 22. The grease samples were evenly placed between the measuring plate and the measuring spindle. The apparent viscosity was tested in rotational mode at shear rates from 0.1 s-1 to 1000 s-1 at room temperature 24 °C.

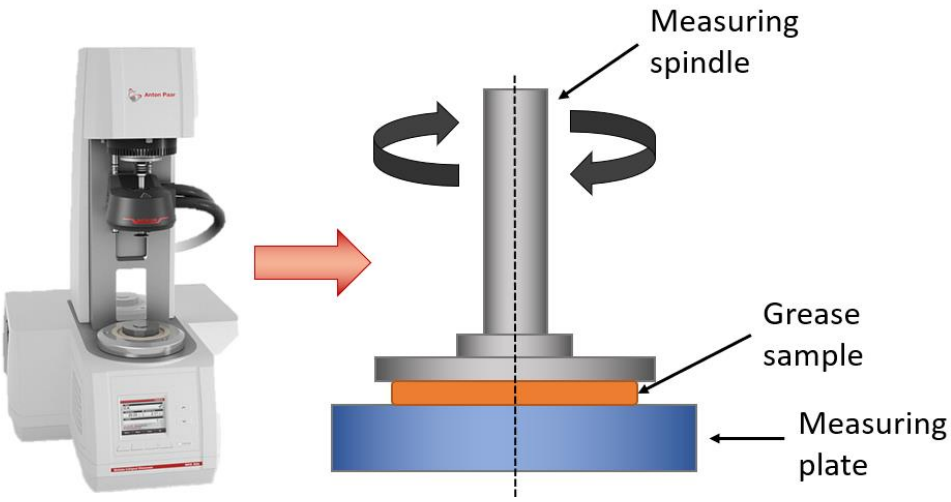


Fig. 22 Rheometer

## 5.2 Experimental methods

### 5.2.1 Colorimetric interferometry

One of the main optical methods used was colorimetric interferometry [93] which allows quantitative evaluation of the distribution of the lubricating film thickness in the EHD contact. The principle of the method is based on the interference of incoherent white light. When illuminated, one part of the incident beam is reflected from a thin chromium layer located on the underside of the disc. The other part of the beam continues through the chromium layer and reflects off the surface of the sphere. A schematic of the method is shown in Fig. 23. The resulting shift of light results in interference, more precisely a change in the intensity and colour of the light. The subsequent calibration of the method consists of taking a monochromatic and a chromatic image of the same static contact and assigning specific thicknesses to the light interference. The monochromatic interferogram is used to define the geometry covered by the colour palette obtained by statistical analysis processing of the chromatic interferogram. A more detailed description of the method can be found, for example, here: [94]. A CCD digital camera is used to take the images and a mercury lamp is used as the light source. To increase the measurement range, a trichromatic source containing light from three diodes can be used. These sources produce light of a certain wavelength intensity and allow a much larger range of interference measurements. This range can then be used up to a thickness of 1500 nm. A range using white light allows measurements up to 900 nm. This method is implemented in the computer program ACHILES. The resolution of colorimetric interferometry is 1 nm.

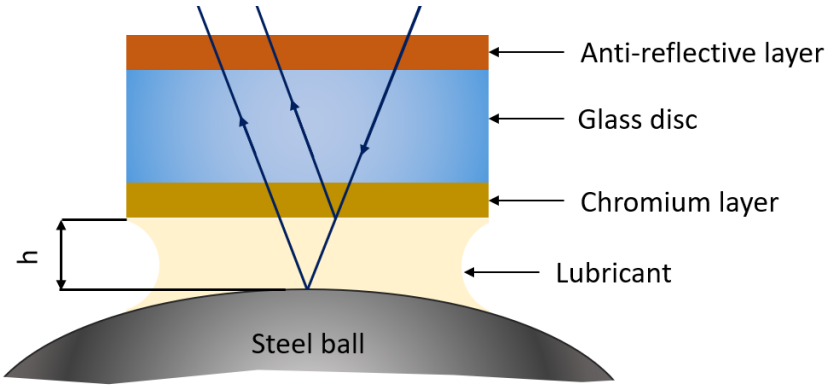


Fig. 23 The origin of optical interferometry at the disc-ball interface

The colorimetric interferometry method has its limitations, which were taken into account in the experiments. The method uses reflection from a reflective surface, so it does not allow measurements with materials that do not produce a reflection. Another significant limitation of the method is the inability to measure thickness on a single surface and it is always necessary to measure thickness between two surfaces. Therefore, the method was only used for measurements in the contact area. Another limitation is the chrome coating, which rubs off during sliding. Therefore, it was necessary to maintain clean rolling conditions during long term experiments. It is for this reason that the coating was not applied to the groove in the ball-on-ring device, where the coating would have been affected during the experiment and the measured thickness affected. The spherical coating makes this task even more complicated.

### 5.2.2 Fluorescent microscopy

Fluorescence microscopy was the other main observation method used. This method can be used on the same optical tribometer as the calorimetric interferometry method but this method does not use the coating of glass disks. Fluorescence microscopy does not primarily use the wave property of light as in the case of optical interferometry, but focuses on using the intensity of light. The phenomenon of fluorescence consists of several sub-phenomena which, for example, are described by Lakowicz [95]. The main principle of the method is based on the exposure of a fluorescent dye to light of a specific wavelength. The dye emits light of a new wavelength in response to excitation Fig. 24. The difference between the wavelengths is called the Stokes Shift. So, the first step is excitation which is caused by the photon delivering energy to the fluorescent dye. Then the Excited-state lifetime occurs, which lasts in the order of nanoseconds. During this time, the dye molecule undergoes relaxation (energy dissipation). A photon is then emitted while the fluorescent molecule returns to its original state. Due to the previous energy dissipation, the photon then occurs in a lower energy state and thus has a longer wavelength than the excited light source.

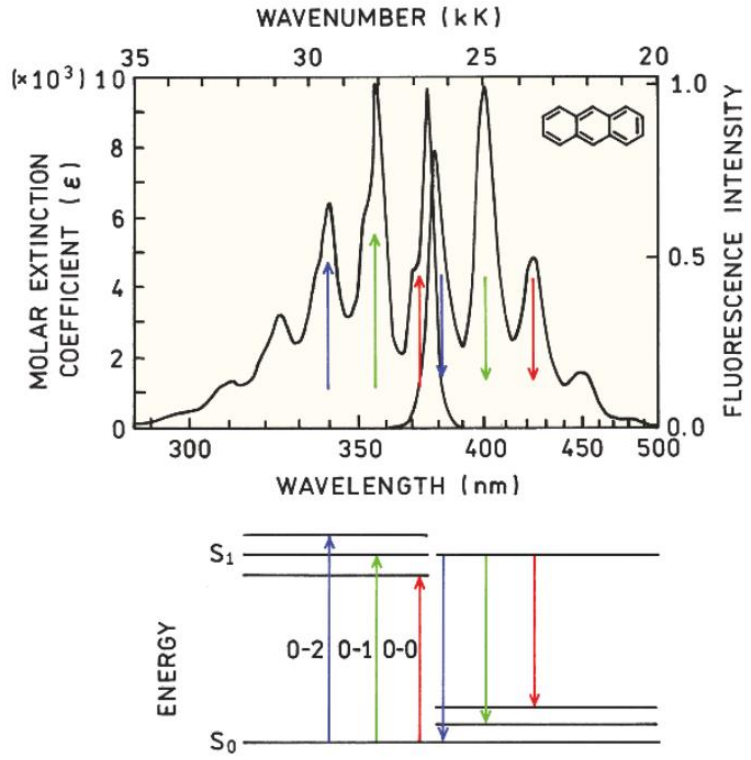


Fig. 24 Absorption and fluorescence emission spectra for anthracene [95]

To use the fluorescence microscopy method, the fluorescent dyes Pyrene and Coumarin 6 were used in this work. A schematic of the fluorescence excitation and emission spectra are shown in Fig. 25. These are dyes that are commonly used for mapping lubricating films [96]. For the excitation of Pyrene, a UV lamp with a wavelength of 330 nm was used and for the excitation of Coumarin 6, a Led diode with a wavelength of 415 nm was used. For filtering the emitted light, a fluorescence filter assembly was used to filter out unwanted light components. A Nikon 91020 TE 2000 was used for Pyrene and a 49000 Et-DAPI for Coumarin 6. An Andor Neo 5.5 camera with a CMOS sensor was used to capture the emitted radiation. For point excitation, an aperture was added to the optical path to limit the viewing area.

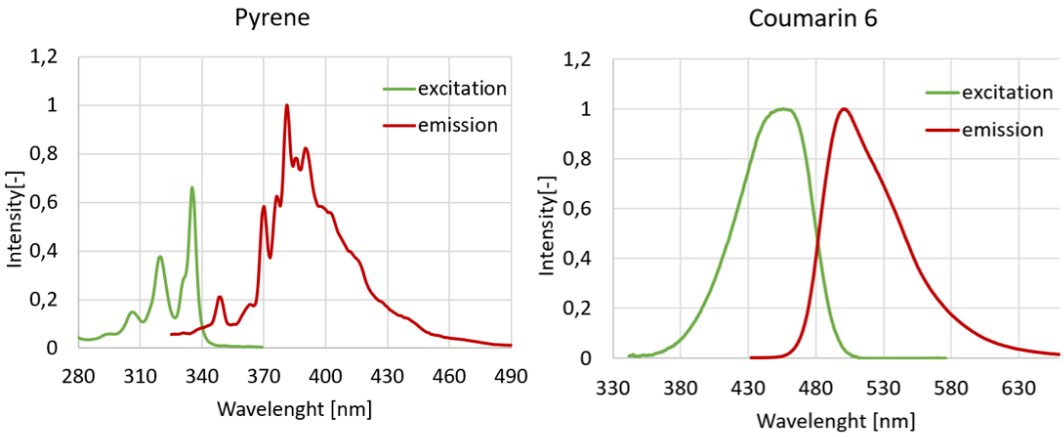


Fig. 25 Pyrene and Coumarin 6 fluorescence spectre

Fluorescence microscopy has several limitations. The first major limitation is the quenching effect of the fluorescent dye. The first source of this effect is prolonged exposure to excitation radiation. The dye shows a gradual decrease in intensity with prolonged exposure. Therefore, a short exposure time to the dye was necessary in the experiments. Another source of the quenching effect may be contamination by chromium particles, which has been presented in several publications [97,98]. Therefore, validation experiments were performed to measure the thickness using interferometry. It was shown that the fluorescence intensity under pure rolling conditions is not affected by this negative effect. Another negative effect is the light interference that occurs at the edges of the contact area. Therefore, the intensity was always sensed in the central region. Another negative effect is the sensitivity to ambient light, (parasitic from the environment, illumination of a larger viewing area) Therefore, spot exposure was used for the film thickness measurements and the entire contact simulator was placed in a shielding tent.

### 5.2.3 Capacitance method

The electrical capacitance method was used to measure the thickness of the lubricating film in the deep groove ball bearing. As shown in the schematic of Fig. 21the bearing is inserted into the electrical circuit and the capacitance is then measured by lubricating the outer and inner ring. The measured electrical capacitance includes the contribution of the EHL contacts as well as the background capacitance, which is unchanged during the measurement. The lubricating film formed then only affects the capacitance formed in those EHL contacts. This method was published by Jablonka et al. [84,86]. The individual contacts are then treated as small parallel plate capacitors ($A_{Hertz}$) separated by a dielectric, compressed oil, with thickness ($h_c$). The capacitance is then given by:

$$C_{Hertz} = \frac{\epsilon_0 \epsilon_{0il} A_{Hertz}}{h_c}$$

where ($\epsilon_0$)is the permittivity constant ($8{,}85\times10^{-12}$ F/m), ($\epsilon_{oi}$)l is the dielectric constant of the dielectric material. This value needs to be augmented by the contribution to the capacitance that is due in the vicinity of the Hertzian contact, which is here called the "outside capacitance", The outside capacitance has two regions, one at the inlet of the contact filled with oil ($C_{Flooded}$ ) and the other at the outlet of the contact where layers of oil separated by air fill the gap between the contacts. ($C_{cav}$). Therefore, the external capacitance can be calculated as:

$$C_{Out\ side} = C_{Flooded} + C_{Cav}$$

$C_{Flooded}$ and $C_{cav}$ are given by relations:

$$C_{Flooded} = \iint_{A_{Flooded}} \frac{\epsilon_0 \epsilon_{0il} dxdy}{h_c + h_{gap}\,(x,y)}$$

$$C_{Cav} = \iint_{A_{Cav}} \frac{\epsilon_0 dxdy}{\frac{h_c}{\epsilon_{0il}} + h_{gap}\,(x,y)\frac{1}{\epsilon_{Air}}}$$

where ($h_c$)is the central film thickness and ($h_{gap}$) is the distance between the ball and the ring from the Hertzian contact. Then, for a radial ball bearing with n rolling elements which is axially loaded, a electric circuit connecting rings with n capacitors arranged in parallel is formed. But under the assumption of creating the same layer thickness on each rolling element. The capacitance between the rolling element and the inner ring equals:

$$C_I = C_{i,Hertz} + C_{i,Outside}$$

And for contact with the outer ring:

$$C_I = C_{i,Hertz} + C_{i,Outside}$$

For a number n of the rolling element, the capacity of the inner ring is:

$$C_{inner} = nC_i$$

and the capacity of the outer ring is obtained by the formula:

$$C_{outer} = nC_o$$

The capacities of the inner and outer rings are in series and therefore the total bearing capacity is given by:

$$C_{Hertz} = \frac{1}{\frac{1}{C_{inner}} + \frac{1}{C_{outer}}} + C_{Backround}$$

To calculate the thickness in an axially loaded radial ball bearing lubricated with grease, it is necessary to include the starvation effect, which affects the amount of lubricant at the inlet

to the contact and therefore the outside capacity. This extension was developed by Shetty in his publication [71] where the method is introduced in more detail. To calculate the external capacitance, the meniscus position parameter m was included, which can be obtained using the Hamrock and Dowson equations for the film thickness in the starved contact [22].

Capacitive methods have limitations even when measuring thin layers. When measuring layers thinner than 100 nm, the electric current through the contact is discharged and the measurement is affected. Therefore, experiments had to be performed from higher ranges, for example from 100 rpm. At higher speeds, a greater layer thickness was achieved and the effect of breakdown was no longer observed.

## 5.3 Experiment design and methodology

### 5.3.1 Paper A

This publication focuses on the method of dyeing individual components of grease with fluorescent dyes and subsequent independent observations. Ball-on-disc and Ball-on-ring simulators were used to verify the applicability of the method. For both devices, a 25.4 mm diameter ball made of 100CR6 chromium steel and a disc/ring made of BK7 were used. The experiments were performed under pure rolling conditions and at the same contact pressure of p = 0.3 GPa.

A general multipurpose grease with a lithium complex thickener and PAO8 base oil was used. PAO8 base oil was chosen because it has no natural fluorescent properties. The viscosity of this base oil is 46.2 cSt at 40 °C. The NLGI class of the grease produced is 2. Two dyes were used in this grease - Coumarin 6 and Pyrene. Coumarin 6 was used to monitor the thickener and pyrene was used to monitor the base oil. The content of Coumarin 6 was 200 ppm and content of pyrene was 1 wt.%, respectively. Both dyes were dissolved in PAO8 base oil at elevated temperature prior to manufacturing the grease. After complete dissolution, the grease was formulated in a conventional manner.

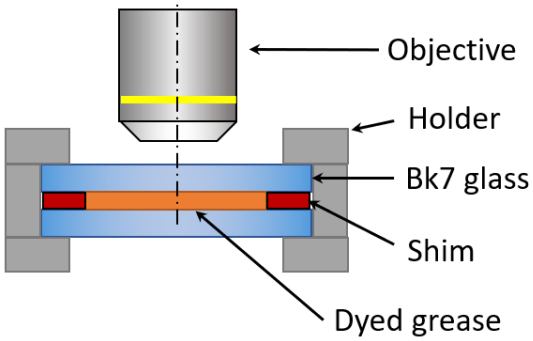


Fig. 26 Diagram of the calibration assembly.

First, a series of tests were carried out to prove that the ratio of fluorescence emission of Coumarin 6 and Pyrene, i.e. from the thickener and the oil. A sandwich calibrator Fig. 26 with a 50 μm gap created by a metallic shim was used and also images were taken without the gap. Due to the different concentrations and different dye strengths, the signal from Pyrene was amplified approximately 4.8 times, achieving a similar signal strength to that of Pyrene. This is considered a calibration because the sum of the fluorescence obtained from Pyrene and Coumarin 6 together is now 84% from pyrene and 16% from Coumarin 6. The original distribution of thickener and base oil was 84 % oil and 16 % thickener.

Subsequently, tests were performed to compare the optical distortion of the devices shown in Fig. 20 The glass ring can produce optical distortion because it has curved surfaces on the outside and inside. Therefore, a series of images were taken of a ball with specific roughening on the outside of the ring and in contact with the ring, and then the images were compared.

Subsequently, a comparative measurement was made at 1.42 mm/s on the Ball-on-disc and Ball on Ring devices to observe the different behaviour of the grease components around the EHL contact. After the break, it was always possible to observe that the two lubricant components had separated and a more efficient replenishment of the conformality 0,58 created by the Ball-on-ring device was observed.

### 5.3.2 Paper B

The second publication focuses on an experimental study of grease replenishment at different contact conformities. The aim was to show how the change in conformality affects the natural lubricant replenishment and the level of starvation. Subsequently, the contact areas and the resulting rolling paths were observed. The work focused on the assessment of base oil continuity and grease behaviour. Therefore, a dyed base oil was used in the grease lubricant and a pure base oil was also used for comparison. An experimental setup in ball on ring configuration and different rolling elements were used for the tests. The list of rolling elements used is given in Table 1. The glass ring has a groove with a radius of 13.2 mm. The different diameters of the rolling elements and the groove in the ring then simulate the actual conformity of a deep groove ball bearing.

Table 1 Specifications of rolling elements.[99]

| Ball diameter [mm] | Conformity (f) [-] | Ellipticity of contact [-] |
|---|---|---|
| 25.4 | 0.52 | 8.4 |
| 23.8 | 0.55 | 4.5 |
| 22.2 | 0.58 | 3.3 |

All rolling elements were made of chrome steel 100CR6 and were optically smooth (Ra < 6 nm). The experiments were performed at a contact pressure of 0.3 GPa. The temperature during the experiment was approximately 26 ± 0.5 °C and the range of speeds tested was 0-2 m/s. Multiple regions were observed during the experiments. First, a region providing direct information about the amount of lubricant in the contact area (0.5 x 0.2 mm). The second area observed included information about the area around the contact and meniscus (8 x 1.6 mm). In addition to the area around the contact, the path behind the contact was also observed, where an equally large area was observed. This observation linked the formation of the lubricant film thickness in the contact and the amount of lubricant in the surrounding area. The grease used for the experiment was a lithium complex grease Table 2. This lubricant contained the fluorescent dye pyrene. The dye was applied only to the base oil in the lubricant. The content of the fluorescent dye was 1 wt. %. The dye was also applied to the base oil itself, for comparative measurements. The same calibration procedure as in the previous publication was used for thickness calibration Fig. 26.

Table 2 Properties of used samples [99]

| Grease property | Grease 1 | Mineral base oil |
|---|---|---|
| **Recommended operating temperature [°C]** | -30 to +120 | -30 to +120 |
| **NLGI Grade [-]** | 2-3 | - |
| **Base oil kinematic viscosity at 40 °C [$mm^2s^{-1}$]** | 50 | 50 |
| **Penetration at 25 °C (ISO 2137) [10-1 mm]** | 270 | - |
| **Thickener** | Li-soap | - |

In the experiments with grease, a quantity of 0.5 g was always used. This amount was always weighed and then gradually applied to the rolling element. During the application of the sample, the ball was in contact with the ring, which was rotated at a speed of 5 revolutions per minute. The application was carried out gradually, with one revolution applying the full amount of lubricant to the groove in the ring. A micropipette was used for the base oil experiments. The lubricant was applied sequentially into the groove in the ring, which was rotated at 5 revolutions per minute.

### 5.3.3 Paper C

The third publication focused on the behaviour of the thickener in EHL contacts. The aim was to demonstrate the ability of the thickener to contribute to lubricant film formation under different kinematic conditions. Two types of thickeners with different structures Table 3 were tested. The lubricants did not contain any additives but contained the fluorescent dye Coumarin 6. The concentration of the fluorescent dye Coumarin 6 used was 200 ppm. The dye was first mixed in the base oil and then other substances were added to the oil to form a thickener. Due to the more polar chemical properties of the thickener and dye, the dye was bound to the thickener. The structure of the thickener was analysed using an electron microscope and is shown in Fig. 27. Each sample was washed with hexane and then filtered. After washing out the base oil, the thickener itself remained. Subsequently, the samples were scanned using a microscope.

The samples were tested for concentration under fully flooded and starved conditions. Ball-on-disc experiments were performed first, followed by Ball-on-ring experiments to verify the interconnectivity of the two systems. Colorimetric interferometry and fluorescent microscopy in identical tests were used to determine the representation of the thickener.

Table 3 Properties of used samples [100]

| **Grease property** | **Grease A** | **Grease B** | **Grease C** |
|---|---|---|---|
| **Base oil type** | Poly-alpha-olefin (PAO) | Poly-alpha-olefin (PAO) | Poly-alpha-olefin (PAO) |
| **Viscosity of base oil N ($mm^2 \cdot s^{-1}$) at 40 °C** | 46 | 46 | 46 |
| **Thickener type** | Alicyclic di-urea | Alicyclic di-urea | Lithium complex |
| **Thickener concentration (wt%)** | 15 | 15 | 16 |
| **Penetration (60W)** | 275 | 226 | 268 |
| **Density of the grease ($g/cm^3$)** | 0.85 | 0.84 | 0.85 |
| **Average diameter (µm)** | ≈0.04 | ≈0.04 | ≈0.13 |
| **Structure after homogenisation** | Normal | Fine | Normal |

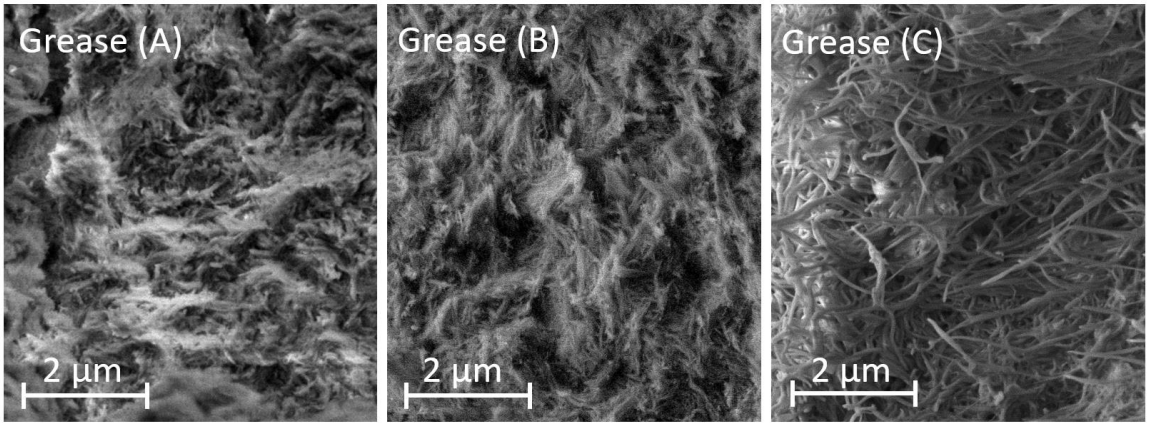


Fig. 27 SEM images of grease thickener fibres [100]

First, experiments were performed on a device with a ball-on-disc configuration at a velocity of 100 mm/s and a contact pressure of 0.3 GPa. The experiments were first conducted under fully flooded conditions, where the wiper artificially added lubricant to the contact and the contact area was observed during rotation. A series of experiments were always performed in which the film thickness for a given lubricant was first measured using interferometry. Then the experiment was repeated and the intensity of the dye trapped on the thickener was measured by fluorescence microscopy. The calibration of the fluorescence data was the same as in the previous publication Fig. 26. Comparison of the two observational approaches was then used to determine the concentration of thickener in the lubricant film. Further experiments were performed at 100 mm/s but without artificially directing the lubricant into the path. This created starvation conditions after the first rotation of the disc. Again, both observation methods were used and again the evolution of the thickener concentration was determined. Then, experiments were performed for different speeds on the lubricant (B), namely 25 mm/s, 50 mm/s, 100 mm/s, 200 mm/ under fully flooded conditions.

The next part of the publication focused on the experiment with the Ball-on-ring device and the subsequent comparison with the Ball-on-disk device. The experiments were conducted at a constant pressure of 0.3 GPa with a ball size of 25.4 mm and a conformality of 0.52. The experiments were conducted for speeds of 25 mm/s, 50 mm/s, 100 mm/s, 200 mm/s, where no artificial lubricant was introduced into the contact. For each experiment, 0.5 g of fresh lubricant was used and applied to the ball at a speed of 5 rpm and evenly applied to the track during the first revolution. The amount of lubricant was always weighed using a balance. Fluorescence microscopy was used to measure the intensity in contact and to observe the surroundings afterwards. The effect of the actual geometry of the radial ball bearing on the behaviour of the thickener in the EHL contact and its surroundings was then evaluated by comparing the results from both devices.

### 5.3.4 Paper D

The fourth publication focused on linking the findings of the Ball-on-disc tribometer with radial deep groove ball bearings. The film thickness in axially loaded ball bearings can be described by the product of the base oil viscosity, half contact width and speed (ηbu). However, observations from previous publications show the influence of the thickener on the film thickness. Therefore, experiments under the same contact and velocity conditions were performed on a Ball-on-disc tribometer and a radial deep groove ball bearing with the selected samples Table 4. Samples with the same base oil but with different types of thickener were used, showing different behaviours. The concentration of thickener was very similar and around 15% and the samples did not contain any additives. The results were further compared with a prediction theorem describing the evolution of the normalized film thickness.

Table 4 Properties of used samples

| Grease property | Grease (Alic.) | Grease (Lith.) | Grease (Alip.) |
|---|---|---|---|
| **Base oil type** | Poly-alpha-olefin (PAO) | Poly-alpha-olefin (PAO) | Poly-alpha-olefin (PAO) |
| **Viscosity of base oil N ($mm^2 \cdot s^{-1}$) at 40 °C** | 46 | 46 | 46 |
| **Thickener type** | Alicyclic di-urea | Lithium complex | Aliphatic di-urea |
| **Thickener concentration (wt%)** | 15 | 16 | 15 |
| **Penetration (60W)** | 275 | 268 | 221 |
| **Density of the grease ($g/cm^3$)** | 0.85 | 0.85 | 0.84 |
| **Structure after homogenisation** | Normal | Normal | Normal |

Ball-on-disc tests were only conducted under fully flooded conditions, with the wiper directing the lubricant pushed out of the contact back into the contact. The tests were carried out at speeds of 330 mm/s, 550 mm/s and 826 mm/s. The contact pressure used was always 0.9 GPa. The evaluation method was colorimetric interferometry. The test time was 7 h of continuous measurement at constant speed. The ambient temperature during the experiment was 24 ± 0.5 °C. To increase the measurement range, a trichromatic led light source was used instead of white light. This change allowed to increase the range of fringing from 900 nm to 1500 nm. A ball with a diameter of 25.4 mm and a roughness of up to (Ra < 6 nm) was used for the experiment. The grease was always evenly applied to the disc before the experiment started. The amount of sample was 2 g.

For the bearing experiment, bearing 6209-2Z was used, which was filled with the tested grease up to 30% of the inner volume. The calibration was first performed using bleeding base oil, which was obtained from the test samples using a centrifuge. The bearing was flooded with the base oil and measurements were taken corresponding to the tested speed and load of 200 N. Then tests were carried out with the grease over a speed range of 120 200, 300, 400, 500, 600 and 700 rpm and the bearing was operated for 24 hours for each speed. For each speed, the bearing was cleaned and new grease was applied. A single-fill test was then performed where all speeds were tested without cleaning the bearing. The bearing first went through a run-in phase at 4000 rpm for 24 h. It was then slowed to 120 rpm, at which it operated for 24 h. Thereafter, the tested speed was increased every 24 h to a final value of 700 rpm. The measured values were then compared with a prediction relationship based on the parameters base oil viscosity, half contact width and speed (ηbu). The rotational speeds of 120, 200 and 300 rpm are equivalent to contact linear speeds of 330 mm/s, 550 mm/s and 826 mm/s respectively (so, similar to the ball-on-disc experiments). The tested range of 120, 200 - 700 rpm corresponds to ndm (speed times mean diameter of the bearing) values of 10,200, 17,000 and 60,000 mm/min.

# 6 RESULTS AND DISCUSSION

This work aims to experimentally study the individual components of grease in radial ball-bearing EHL contact, focusing on their contribution to the resulting lubricating film. The first part used a method of dyeing the individual grease components with fluorescent dyes and observing them separately. This method was then applied to investigate the behaviour of the base in and around the contact in the radial ball bearing geometry at different contact conformities. The method was also used to study the behaviour of the thickener in EHL contacts under different kinematic conditions, comparing its behaviour in a simplified tribometer ball-on-disc geometry and a contact ball bearing geometry. Subsequently, experiments were performed with real ball bearings, where the results were compared with previous publications and available prediction relations to determine the normalized film thickness in the EHL contact. The findings from these experiments can help in designing greases and understanding their behaviour in ball bearings.

The first step was to develop a methodology for dyeing the individual components of grease. **Publication A** presents this methodology, which involves dyeing the individual grease components and subsequently observing them independently. The methodology is based on the use of two fluorescent dyes (Coumarin 6 and Pyrene) that exhibit different binding affinities to the grease components. Grease consists of a polar thickener and a non-polar base oil, and their differing polarities prevent them from mixing. During the grease manufacturing process, the fluorescent dyes, which have different polarities, are mixed in. This difference ensures that each dye binds only to one component of the grease.

The dye Pyrene has been used multiple times in previous publications [96,101]. It has been shown to successfully dye the base oil. However, thickeners in grease appear in larger clusters after manufacturing, which become more homogenized during operation. These structures contain some base oil, and thus, also contain the Pyrene dye. Coumarin 6 was used to dye the thickener. Calibration images from the sandwich test Fig. 26 showed changes in the ratio of the two components. In the peripheral areas of the grease sample, Pyrene was observed at 98% and Coumarin at a few percent. In larger thickener clusters, the signal from Coumarin was around 35% and from Pyrene 65%. When observing larger areas, the distribution matched the original composition of the base oil and thickener in the grease. Therefore, using the two dyes mentioned above, the individual components of the grease can be observed separately, but quantification directly depends on the structure of the grease sample. This structure will change during the experiment, as will the concentration of the individual grease components. It was found that by observing larger areas, the average distribution of components can be determined, which matches the original sample composition. This averaging is sufficient to determine the concentration of both grease components in the lubricating film.

For **Publication B,** the base oil was dyed in the grease and subsequently observed. The behaviour of the base oil was examined in and around the contact at conformities of 0.52, 0.55, and 0.58. Measurements of the film thickness in EHL contact showed good agreement with theoretical calculations and with measurements of the base oil itself. The largest difference was observed during starvation, which accentuated the differences between the conformities. Contacts with higher conformity exhibited more efficient lubricant replenishment and greater film thickness. Subsequent observations of the surroundings showed the opposite trend in the amount of lubricant around the contact. Contacts with lower conformity had a greater amount of lubricant around the contact and on the track compared to contacts with higher conformity. In all cases, the amount of lubricant around the contact was less than 1% of the initially applied lubricant.

The results confirm the effect of conformity on film thickness and lubricant replenishment. The key difference is the greater capillary effect at more conformal contacts, which helps form a meniscus before contact. Although lower conformity produces a narrower contact and therefore less lubricant spreading, the capillary effect is more pronounced. Comparative experiments with base oil and lithium grease showed consistency and confirmed previous observations on ball bearings[69,70]. Only the rheological properties of the base oil can be used to predict the thickness for these greases. However, differences were observed when comparing results and trends between ball bearings and tribometer in ball-on-ring configuration. The normalized thickness in the ball-on-ring configuration was less than that in the ball bearing. This difference was likely due to the different kinematics of the two systems, with the outer ring rotating in the tribometer, which did not contain an inner ring or cage. In the ball bearing, the inner ring rotated while the outer ring was static. Consequently, there was less efficient lubricant replenishment due to the absence of spin and better lubricant redistribution due to the cage. These features were not needed for the conformity comparison. Comparison of the results of the base oil and grease measurements showed good agreement, although the amount of lubricant applied to the raceway had an effect with the base oil. This indicates another difference from measurements on actual bearings, where Shetty[89] states that the amount of lubricant overdosing does not affect the normalized film thickness. In the ball-on-ring measurements, it was noticeable that this difference decreased with increasing speed, and the duration of the experiment was significantly shorter than measurements on real bearings. Thus, the findings **refute *hypotheses H1.1* and *H1.2* but confirm *hypothesis H1.3.***

A prior publication detailed a comparative experiment involving a lithium grease and its base oil. The results indicated that the oil predominantly influences the grease's behavior in EHL contact, aligning with established theories. **Publication C** focused on the behaviour of another type of thickener in this context, comparing it to lithium grease with the same type of base oil and percentage of thickener. According to the literature, urea behaves differently in these scenarios. Two levels of homogenization were prepared to demonstrate the structural effects mentioned in the literature. The aim of Publication C was to conduct comparative

measurements between a tribometer in a ball-on-disc configuration and the actual contact geometry of a ball bearing. Using a combination of fluorescence microscopy and optical interferometry, the concentration of the thickener was determined under fully flooded and starved conditions, and the results were compared with the ball bearing geometry.

Under fully flooded conditions on the ball-on-disc tribometer, it was evident that the lubricating film for alicyclic di-urea grease was significantly thicker than that for lithium grease. A higher degree of homogenization resulted in less fluctuation in film thickness and an increasing trend was observed. Under starved conditions, the film thickness was also greater for the alicyclic grease. When comparing the concentration of thickener under starved and fully flooded conditions, it was observed that the thickener was more prominent under starved conditions. Thickener adherence was more pronounced at slow speeds but also occurred at higher speeds. The adhesion process exhibited a linear character in the initial operating speeds. Thus, the adhesion depended on the amount of fresh lubricant available and its texture. In the case of large clumps, a larger film and thicker layers were formed on the track. However, the actual bearing contact geometry showed less ability to form a thickener layer than the fully flooded conditions of the ball-on-disc device.

The greater film thickness in the case of alicyclic grease was due to the higher concentration of thickener in the lubricating film. The higher concentration resulted in both the formation of a thicker lubricating film and the entry of larger clumps of thickener into contact. The main reason for this is the lower affinity to the base oil and better adhesion properties. It was observed that higher speeds caused less thickener adhesion, while the slow speeds resulted in the greatest adhesion. This speed was also mentioned in the literature as the transient speed, where the film thickness in the contact is as large as the diameter of the thickener fibers. In the case of lithium grease, the film thickness approached that of the oil during the experiment, but increased for alicyclic urea. The real bearing contact geometry exhibited similar trends to the fully flooded conditions of the ball-on-disc configuration. This is due to more efficient replenishment of lubricant around the contact. However, lubricant film formation was more limited due to the limited amount of lubricant around the contact being mechanically processed. In the case of ball-on-disc, fresh lubricant is continuously dispensed into the contact, resulting in more pronounced thickener layer formation. At higher speeds, layer formation was also observed, but only up to a certain point, after which stagnation occurred. The reason for this was the stabilization of the meniscus before contact, i.e., the replenishment of lubricant. At higher speeds, there is less re-flooding of the contact, which limits the amount of thickener that can adhere to the contact surfaces.

Although there is a consensus that the rheological properties of the base oil are most critical for the formation of the lubricating film in bearings and that the calculation of this film thickness after bearing break-in is not based on the thickener, experiments demonstrate the effect of the thickener in both simplified and ball bearing contact geometries. The reason for this difference may be attributed to the higher operating speeds of the ball bearings. The

tribometer experiments were conducted at tens of RPM, while typical operating speeds are in the range of thousands of RPM. This higher speed results in greater shear stresses that can disrupt the structure of the thickener, thereby reducing its influence on film thickness. Additionally, there may be significantly greater starvation conditions at these speeds, where contacts are lubricated with less lubricant, diminishing the potential impact of the thickener. Another limitation is the lack of testing with alicyclic urea greases, as the experiments mainly focused on lithium greases, which, according to both experiments and theory, behave primarily based on the base oil. This might also be due to the shorter experimental duration, where bearings are typically tested for tens of hours, whereas tribometer experiments last only tens of minutes. Consequently, the effect of the thickener may be time-limited and potentially negligible in real applications.

Therefore, it can be concluded that the effect of the thickener is observable and that the film thickness in ball bearing contacts is influenced by the thickener. However, the transferability to radial ball bearings still needs to be verified, as the test conditions and duration may not accurately reflect real conditions. Nonetheless, it is evident that the sticking process occurs over a range of speeds rather than at a single speed and exhibits a linear behaviour during the initial phase of operation. **Hence, hypothesis H2.1 has been confirmed. However, hypothesis H2.2 was disproved** because the actual geometry allows only a small amount of lubricant to be retained near the contact, which is mechanically processed, thus limiting the formation of the thickener layer compared to the ball-on-disc configuration in tribometer tests.

The latest publication **(Publication D)** builds on the previous one and extends the testing to experiments with real bearings. Test conditions shown in previous experiments to be favourable for thickener formation on the track, specifically slow bearing speeds, were selected: 120, 200 - 700 rpm corresponds to ndm (speed times mean diameter of the bearing) values of 10,200, 17,000 and 60,000 rpm The contact pressure was 0.9 GPa and the temperature was room temperature. Measurements were taken both during and after the churning phase to observe the effect of the thickener after the reservoirs were formed. During the churning phase, there is increased movement of the lubricant across the bearing, resulting in fully flooded conditions where the effect of the thickener is most pronounced. Identical experiments were performed with an optical tribometer in a ball-on-disc configuration.

It was shown that an alicyclic di-urea grease forms a larger film than lithium or aliphatic grease, and a gradual increase in film thickness could be observed in contact with the ball-on-disc device. This increase lasted several hours and was similar across the three test speeds. After stopping, a thickener layer on the track was observed, measuring around 500-550 nm. The aliphatic grease also formed a layer, but it was much smaller, around 100 nm. In the experiments with real bearings, the same and higher speeds were tested. A good agreement was observed at low speeds, with a deviation in measurements at higher speeds. When the measurements were fitted with an exponential relationship based on $\eta bu$,

discrepancies were noted for both alicyclic and aliphatic greases, while good agreement was found with lithium grease. Similar trends were observed after the churning phase.

As mentioned earlier, the lower affinity of the thickener causes it to stick to the tracks. The fact that this increase could also be observed in the ball bearing confirms that the thickener is involved in the lubrication processes within the bearing and influences the resulting film thickness. However, the film thickness in the ball bearing is less than that observed in the ball-on-disc tribometer at higher speeds. This may be due to contact starvation occurring in the ball bearing. As shown in Publication C, the limited amount of lubricant near the contact leads to a more restricted formation of the thickener layer. The spin of the balls and the cage effect aid in greater replenishment, and combined with the churning phase, there is enough thickener around the contact to make the mechanisms similar to those in a ball-on-disc configuration with artificial replenishment. Similar trends were measured after bearing break-in, but the thickness was slightly less. This may be due to less thickener on the track or mechanically worn thickener damaged by shearing during the churning phase. A check of the apparent viscosity of the grease sample showed that greases forming a larger film paradoxically have a lower apparent viscosity than those forming a thinner film. When the ball bearing temperature was measured, it was evident that the temperature for all three grease samples was almost the same. Thus, the type of thickener was the only parameter changed that could affect the film thickness in the ball bearing. However, the growth of the thickener layer on the track is finite and stagnates after some time. The stagnation of layer growth may be due to the increasing distance of the layer surface from the surface on which it is formed. As the distance increases, the attractive force of the surface decreases. Another cause may be a decrease in the strength of the layer as it thickens.

The main findings from Publication D show that the low operating speeds in the bearing are comparable to the lubricant behaviour in a ball-on-disc configuration, **thus confirming hypothesis H3.1. However, hypothesis H3.2 has been disproved**, as the thickener remains dominant even at speeds higher than the transit speed.

*The content of pages 56-71 corresponds to Paper [A]*

*https://doi.org/10.1007/s11249-022-01671-7*

Tribology Letters (2022) 70:126
https://doi.org/10.1007/s11249-022-01671-7

TRIBOLOGY METHODS

# Novel In-Situ Observation of the Grease Constituents in Elastohydrodynamic Contacts by Fluorescence Microscopy

David Kostal[1] · Michal Okal[1] · Josef Fryza[1] · Ivan Krupka[1] · Martin Hartl[1]

Received: 10 August 2022 / Accepted: 19 October 2022 / Published online: 7 November 2022
© The Author(s), under exclusive licence to Springer Science+Business Media, LLC, part of Springer Nature 2022

*The content of pages 72-83 corresponds to Paper [B]*

*https://doi.org/10.3390/lubricants10110289*

*lubricants*

MDPI

*Article*

# Effect of Contact Conformity on Grease Lubrication

Michal Okal *, David Kostal *, Petr Sperka, Ivan Krupka and Martin Hartl

Faculty of Mechanical Engineering, Brno University of Technology, Technicka 2896/2, 616 69 Brno, Czech Republic
* Correspondence: michal.okal@vut.cz (M.O.); kostal@fme.vutbr.cz (D.K.)

*The content of pages 84-99 corresponds to Paper [C]*

*https://doi.org/10.1007/s11249-024-01874-0*

Tribology Letters (2024) 72:72
https://doi.org/10.1007/s11249-024-01874-0

ORIGINAL PAPER

# Thickener Behaviour in Rolling Elastohydrodynamic Lubrication Contacts

Michal Okal[1] · David Kostal[1] · Kazumi Sakai[2] · Ivan Krupka[1] · Martin Hartl[1]

Received: 26 March 2024 / Accepted: 21 May 2024 / Published online: 4 June 2024
© The Author(s) 2024, corrected publication 2024

*The content of pages 100-112 corresponds to Paper [D]*

*https://doi.org/10.1080/10402004.2024.2431523*

Tribology Transactions

ISSN: (Print) (Online) Journal homepage: www.tandfonline.com/journals/utrb20

# Experimental Study of the Effect of Thickener on the Film Thickness in the Contacts of a Grease-Lubricated Ball Bearing at Low Speed

Michal Okal, David Kostal, Jude A. Osara, Piet M. Lugt, Ivan Krupka & Martin Hartl

**To cite this article:** Michal Okal, David Kostal, Jude A. Osara, Piet M. Lugt, Ivan Krupka & Martin Hartl (11 Dec 2024): Experimental Study of the Effect of Thickener on the Film Thickness in the Contacts of a Grease-Lubricated Ball Bearing at Low Speed, Tribology Transactions, DOI: 10.1080/10402004.2024.2431523

**To link to this article:** https://doi.org/10.1080/10402004.2024.2431523

# 7 CONCLUSIONS

Although the formation of lubricant films in ball bearings is critical to their operation, there are still gaps in understanding the behaviour of greases in ball bearings. This dissertation focuses on the experimental investigation of the individual components of grease lubricants in the EHL contact region of ball bearings. The main findings of this work are summarized below.

It has been confirmed that the behaviour of lithium grease in and around the EHL contact is primarily influenced by the rheological properties of the base oil. It has also been shown that only a small amount of lubricant is actively involved in lubricating the EHL contact in ball bearings, and this depends on the specific contact conformity. More conformal contacts can reduce starvation due to a greater capillary effect, even though there is less lubricant available in the vicinity because of the narrower gap.

The proportion of thickener in the EHL film varies according the type of thickener. For lithium-based thickeners, an effect can be observed only at the initial proving times and then the effect disappears. But the alicyclic di-urea thickener actively participates in the formation of the lubricating film by forming a layer of thickener on the track and hence the thickener has a higher percentage in the lubricating film.

The formation of the thickener layer on the track is influenced by the amount of available grease, with the build-up effect being more pronounced in fully flooded conditions compared to starved conditions. In a contact ball bearing geometry with no additional grease replenishment, the limited grease supply results in a less pronounced build-up of this layer.

At bearing speeds considered very slow [102] , there is a correlation in the lubricating film formation within EHL contacts when compared to tribometers using a ball-on-disc configuration. This agreement arises because fully flooded conditions occur in the bearings, conditions that can also be replicated in tribometers with simplified geometry.

Film formation in ball bearings is influenced not only by the rheology of the base oil but also by the properties of the thickener. When using alicyclic di-urea grease, a thickener layer forms on the raceways, increasing the overall lubrication film. The growth of this thickener layer tends to stabilize after 4-5 hours of operation and can reach thicknesses of up to 550 nm. The growth of the thickener layer is possible even after the bearing has been run-in, but only at slow speeds. As a result, the evolution of film thickness cannot be accurately described using the existing equation based on the parameter $\eta bu$.

The knowledge gained from this investigation of carefully selected grease samples will not only enhance the fundamental understanding of ball bearing lubrication but also deepen the

understanding of the behaviour of selected greases, aiding in the further development of these lubricants.

The knowledge gained during the dissertation research can be applied in many areas. One example is positioning mechanisms, where only small rotations often occur, leaving little room for the formation of a continuous lubricating film. These conditions are conducive to the formation of a thickener layer that separates metal surfaces. Thickener layers are also advantageous in applications where vibration occurs, which can be caused by localized reductions in film thickness.

In general, polyurea greases can be used in applications such as electric motors due to properties like higher oxidation stability at elevated temperatures. For this application, predicting the evolution of film thickness is crucial. However, current prediction models cannot fully account for the thickness behaviour of polyurea greases. This thesis presents research comparing the existing knowledge of lithium grease lubrication with that of polyurea grease. The main contributions of this dissertation can be summarized as follows:

- A methodology that enables independent observation of grease components.
- Insights into the impact of ball bearing contact conformity on grease replenishment and starvation levels.
- Demonstration of the relationship between the Ball-on-disc system and the contact geometry of ball bearings, focusing on the behaviour of the thickener in contact.
- Expanding the knowledge of film formation in ball bearings and highlighting the limitations of current equations describing thickness evolution in radial ball bearings.

## 7.1 Recommendations for future research

- The experiments focused on only three basic types of greases: lithium, alicyclic di-urea, and aliphatic di-urea. Future research could include other types of thickeners and base oils. Greases with different rheological properties are expected to exhibit varied contact behaviour.
- Ball bearing experiments were conducted only for a duration of 24 hours. The effect of the thickener is expected to decrease over longer ball bearing operation times; thus, studies involving extended ball bearing operation would help describe the thickener's impact on lubricant film formation.
- The experiments used greases with 15% thickener. Testing greases with different thickener concentrations would be useful, as higher concentrations are expected to exhibit different levels of starvation and a greater influence on the lubricating film.
- The experiments primarily focused on the processes within the ball bearing contact region. Enhancing the ball-on-ring configuration device with a bearing cage or inner ring

would help replicate more accurate grease lubrication mechanisms. A precise understanding of the real system would improve the description of grease lubrication processes.

- The experiments were conducted under uniform parameters such as room temperature and pressures ranging from 0.3 to 0.9 GPa. It is expected that increasing the tested temperature and load will directly affect the behaviour of the thickener and the grease as a whole. Further extended testing would provide additional valuable information on grease behaviour.
- The method of dyeing the grease components was also tested under limited conditions. The effect of contact pressure is expected to cause changes in the observed fluorescence intensity, leading to inaccuracies in the current calibration. Extending the test conditions and performing validation experiments with another observational method would help to clarify possible inaccuracies.

# 8 LIST OF PUBLICATIONS & OUTCOMES

## 8.1 Publications related to the topic of this thesis

D. KOSTAL, M. OKAL, J. FRYZA, I. KRUPKA, AND M. HARTL, "Novel In-Situ Observation of the Grease Constituents in Elastohydrodynamic Contacts by Fluorescence Microscopy," *Tribol.Lett.*, vol. 70, no. 4, Dec. 2022, doi: 10.1007/s11249-022-01671-7. [IF = 3.2]

(Author's contribution 35 %)

M. OKAL, D. KOSTAL, P. SPERKA, I. KRUPKA, AND M. HARTL, "Effect of Contact Conformity on Grease Lubrication," Lubricants, vol. 10, no. 11, Nov. 2022, doi: 10.3390/lubricants10110289. [IF = 3.2]

(Author's contribution 65 %)

M. OKAL, D. KOSTAL, K. SAKAI, I. KRUPKA, AND M. HARTL, "Thickener Behaviour in Rolling Elastohydrodynamic Lubrication Contacts," *Tribol Lett*, vol. 72, no. 3, p. 72, Sep. 2024, doi: 10.1007/s11249-024-01874-0. [IF = 3.2]

(Author's contribution 70 %)

M. OKAL, D. KOSTAL, J. OSARA, P. LUGT, I. KRUPKA, AND M. HARTL, "Experimental study of the effect of thickener on the film thickness in a rolling bearing at low speeds," *Tribol. Trans.*, vol. 1-13, Dec. 2024, 10.1080/10402004.2024.2431523. [IF = 2]

(Author's contribution 65 %)

# 9 LITERATURE


[1] Lugt, P.M., Grease lubrication in rolling bearings. John Wiley & Sons. 2012.

[2] Lugt, P.M., A Review on grease lubrication in rolling bearings. Tribol. Trans. 2009; 52:470–80. https://doi.org/10.1080/10402000802687940.

[3] Harris, T. A., Kotzalas, M. A., Essential concepts of bearing technology. CRC Press; n.d.

[4] Saatchi, A., Shiller, P.J., Eghtesadi S.A., Liu, T., Doll, G.L., A fundamental study of oil release mechanism in soap and non-soap thickened greases. Tribol. Int. 2017; 110:333–40. https://doi.org/10.1016/j.triboint.2017.02.004.

[5] Hurley, S., Cann, P.M., Spikes, H.A., Lubrication and reflow properties of thermally aged greases. Tribol. Trans. 2000; 43:221–8. https://doi.org/10.1080/10402000008982332.

[6] Roman, C., Valencia, C., Franco, J.M., AFM and SEM assessment of lubricating grease microstructures: Influence of sample preparation protocol, frictional working conditions and composition. Tribol. Lett. 2016; 63. https://doi.org/10.1007/s11249-016-0710-y.

[7] Larsson, E., Westbroek, R., Leckner, J., Jacobson, S., Rudolphi, Å.K., Unraveling the lubrication mechanisms of lithium complex (LiX)- and polypropylene (PP)-thickened greases in fretting – Part I: Fretting experiments and surface analysis. Wear 2022;490–491. https://doi.org/10.1016/j.wear.2021.204192.

[8] Couronne, I., Blettner, G., Vergne, P., Rheological behavior of greases: Part i—effects of composition and structure. Tribol. Trans. 2000; 43:619–26. https://doi.org/10.1080/10402000008982386.

[9] Lugt, P.M., Modern advancements in lubricating grease technology. Tribol. Int. 2016; 97:467–77. https://doi.org/10.1016/j.triboint.2016.01.045.

[10] Chatra, K.R.S., Osara, J.A., Lugt, P.M., The lubrication mechanism behind the transition from churning to bleeding in grease lubricated bearings – Experimental characterization. Tribol. Int. 2023; 183. https://doi.org/10.1016/j.triboint.2023.108375.

[11] Chatra, S., Lugt, P.M., The process of churning in a grease lubricated rolling bearing: Channeling and clearing. Tribol. Int. 2021; 153. https://doi.org/10.1016/j.triboint.2020.106661.

[12] Chatra, K.R.S., Lugt, P.M., Channeling behavior of lubricating greases in rolling bearings: Identification and characterization. Tribol. Int. 2020; 143. https://doi.org/10.1016/j.triboint.2019.106061.

[13] Wikström, V., Jacobson, B., Loss of lubricant from oil-lubricated near-starved spherical roller bearings. Proc. IMechE, Part J: J. Eng. Tribol. 1997; 211:51–5. https://doi.org/https://doi.org/10.1243/1350650971542318.

[14] Lugt, P.M., Velickov, S., Tripp, J.H., On the chaotic behavior of grease lubrication in rolling bearings. Tribol. Trans. 2009; 52: 581–90. https://doi.org/10.1080/10402000902825713.

[15] Larson, R., EHL film thickness behavior - encyclopedia of tribology, Springer, US; 2013; https://doi.org/10.1007/978-0-387-92897-5

[16] Reynolds, O., On the Theory of lubrication and its application to Mr. Beauchamp Tower's Experiments, including an experimental determination of the viscosity of olive oil. Philos. Trans. R. Soc. Lond. n.d.; 177:157.

[17] Meldahl, A., Contribution to the theory of the lubrication of gears and of the stressing of the lubricated flanks of gear teeth. Brown Boveri review. 1941; 28:374–82.

[18] Dowson, D., Higginson, G.R., Whitaker, A. V., Elasto-hydrodynamic lubrication: a survey of isothermal solutions. J. Mech. Eng. Sci., 1962; 4:121–6.

[19] Dowson, D., Higginson, G.R., The effect of material properties on the lubrication of elastic rollers. J. Mech. Eng. Sci., 1960; 2:188–94.

[20] Dowson, D., Higginson G.R., A Numerical Solution to the elasto-hydrodynamic problem. J. Mech. Eng. Sci., 1959; 1: 6–15. https://doi.org/10.1243/jmes_jour_1959_001_004_02.

[21] Hamrock, B.J., Dowson, D., Isothermal elastohydrodynamic lubrication of point contacts - Part III. fully flooded results. J. Lubr. Tech.; 1977; 99:264–76.

[22] Hamrock, B.J., Dowson D. Isothermal elastohydrodynamic lubrication of point contacts. Part 4 - Starvation results. Trans. Asme, Ser F, J. Lubr. Tech. 1977; 99, no.1.:15–23.

[23] Hamrock, B.J., Dowson D. Isothermal elastohydrodynamic lubrication of point contacts Part 1-theoretical formulation. J. Tribol. 1976; 98:223–8.

[24] Hamrock, B.J., Dowson D. Isothermal elastohydrodynamic lubrication of point contacts Part II- eilipticity parameter results. J. Tribol. 1976; 98:375–81.

[25] Nijenbanning, G., Venner, C.H., Moes, H., Film thickness in elastohydrodynamically lubricated elliptic contacts. Wear. 1994; 176:217–29. https://doi.org/10.1016/0043-1648(94)90150-3.

[26] Chevalier, F., Lubrecht, A.A., Cann, P.M.E., Colin. F., Dalmaz. G., Film thickness in starved EHL point contacts. J. Tribol. 1998; 120:126–33. https://doi.org/10.1115/1.2834175.

[27] Kostal, D., Sperka, P., Hartl, M., controlling and measuring starvation 2014; 21:321–8.

[28] Van Zoelen, V., Thin Layer Flow in Rolling Element Bearings. University of Twente, Netherlands 2009; Ph. D. thesis.

[29] Orcutt F.K., Cheng, H.S., Gyro-spin axis hydrodynamic bearing symposium. Lubrication of Rolling Contact Instrument Bearings, 1966; 87.

[30] Wedeven, L.D., Evans, D., Cameron, A., Optical analysis of ball bearing starvation. J. Lubr. Technol. 1971; 93:349–61.

[31] Wolveridge, P.E., Baglin. K.P., Archard, J.F., The starved lubrication of cylinders in line contact. Proceedings of the Institution of Mechanical Engineers 1970; 185: 1159–69. https://doi.org/10.1243/pime_proc_1970_185_126_02.

[32] Chevalier, F., Lubrecht, A.A., Cann, P.M.E., Colin, F., Dalmaz, G., Starvation phenomena in EHL. point contacts: influence of inlet flow distribution. Tribol. Ser. 1996; 31:213–23. https://doi.org/https://doi.org/10.1016/S0167-8922(08)70785-5.

[33] Damiens, B., Venner, C.H., Cann, P.M.E., Lubrecht, A.A., Starved lubrication of elliptical EHD contacts. J. Tribol. 2004; 126:105–11. https://doi.org/10.1115/1.1631020.

[34] Svoboda, P., Kostal, D., Krupka, I., Hartl, M., Experimental study of starved EHL contacts based on thickness of oil layer in the contact inlet. Tribol. Int. 2013; 67:140–5. https://doi.org/10.1016/j.triboint.2013.07.019.

[35] Kostal, D., Sperka, P., Svoboda, P., Krupka, I., Hartl, M., Experimental observation of lubricated contacts replenishment 2015: 640–4. https://doi.org/10.17973/MMSJ.2015.

[36] Cann, P.M.E., Damiens, B., Lubrecht, A.A., The transition between fully flooded and starved regimes in EHL. Tribol. Int. 2004; 37:859–64. https://doi.org/10.1016/j.triboint.2004.05.005.

[37] Van Zoelen, M.T., Venner, C.H., Lugt, P.M., The prediction of contact pressure-induced film thickness decay in starved lubricated rolling bearings. Tribol. Trans. 2010; 53:831–41. https://doi.org/10.1080/10402004.2010.492925.

[38] Venner. C.H., Van Zoelen, M.T., Lugt, P.M., Thin layer flow and film decay modelling for grease lubricated rolling bearings. Tribol. Int. 2012; 47:175–87. https://doi.org/10.1016/j.triboint.2011.10.019.

[39] Chiu, Y.P., An analysis and prediction of lubricant film starvation in rolling contact systems. Tribol. Trans. 1974; 17:22–35. https://doi.org/10.1080/05698197408981435.

[40] Pemberton, J., Cameron, A., A mechanism of fluid replenishment elastohydrodynamic contacts in 1976; 37:185–90.,

[41] Kingsbury, E., Parched elastohydrodynamic lubrication. J. Tribol. 1985:229–32. https://doi.org/https://doi.org/10.1115/1.3261026.

[42] Guangteng, G., Cann, P.M., Spikes, H.A., A study of parched lubrication. Wear 1992; pp 91–105. doi:10.1016/ 0043-1648(92)90263-8

[43] Guangteng, G., Spikes, H.A., The role of surface tension and disjoining pressure in starved and parched lubrication 1996; Proc. IMechE, Part J: J. Eng. Tribol.210(2), pp 113–124. doi:10.1243/PIME_PROC_1996_210_487_02

[44] Jacod, B., Pubiliera, F., Cann, P.M.E., Lubrechta A.A., An analysis of track replenishment mechanisms in the starved regime. Tribol. Ser., Vol. 36, pp 483–492. Elsevier. doi:10. 1016/S0167-8922(99)80069-8

[45] Nogi, T., Film thickness and rolling resistance in starved elastohydrodynamic lubrication of point contacts with reflow. J. Tribol. 2015; 137. https://doi.org/10.1115/1.4030203.

[46] Nogi, T., An analysis of starved EHL point contacts with reflow. Tribol. Online 2015;10:64–75. https://doi.org/10.2474/trol.10.64.

[47] Gershuni, L., Larson, M.G., Lugt, P.M., Lubricant replenishment in rolling bearing contacts. Tribol. Trans. 2008; 51:643–51. https://doi.org/10.1080/10402000802192529.

[48] Van Zoelen, M.T., Venner, C.H, Lugt, P.M., Free surface thin layer flow on bearing raceways. J. Tribol. 2008; 130:1–10. https://doi.org/10.1115/1.2805433.

[49] Fischer, D., Von Goeldel, S., Jacobs, G., Stratmann, A., Numerical investigation of effects on replenishment in rolling point contacts using CFD simulations. Tribol. Int. 2021; 157:106858. https://doi.org/10.1016/j.triboint.2021.106858.

[50] Chong, W.W.F., Teodorescu, M., Rahnejat, H., Rupture and reformation of ultra-thin surface films. 2010: https://doi.org/10.1115/DETC2010-28427

[51] Bruyere, V., Fillot, N., Morales-Espejel, G.E., Vergne, P., A two-phase flow approach for the outlet of lubricated line contacts. J. Tribol. 2012; 134. https://doi.org/10.1115/1.4006277.

[52] Åström, H., Östensen, J. O., Höglund E., Lubricating Grease Replenishment in an Elastohydrodynamic Point Contact. J. Tribol. 1993; 115:501–6. https://doi.org/DOI 10.1115/1.2921666.

[53] Åström, H., Isaksson, O., Höglund, E., Video recordings of an EHD point contact lubricated with grease. Tribol. Int. 1991; 24:179–84. https://doi.org/10.1016/0301-679X(91)90024-4.

[54] Cann, P.M., Starvation and reflow in a grease-lubricated elastohydrodynamic contact. Tribol. Trans. 1996; 39:698–704. https://doi.org/10.1080/10402009608983585.

[55] Cann, P.M., Starved grease lubrication of rolling contacts. Tribol. Trans. 1999;42: 867–73. https://doi.org/10.1080/10402009908982294.

[56] Cen, H., Lugt, P.M., Morales-Espejel, G., On the Film Thickness of Grease-Lubricated Contacts at Low Speeds. Tribol. Trans. 2014; 57:668–78. https://doi.org/10.1080/10402004.2014.897781.

[57] Zhang, X., Glovnea, R., Grease film thickness measurement in rolling bearing contacts. Proc. IMechE, Part J: J. Eng. Tribol. 2021; 235:1430–9. https://doi.org/10.1177/1350650120961278.

[58] Morales-Espejel, G.E, Lugt, P.M., Pasaribu, H. R., Cen, H., Film thickness in grease lubricated slow rotating rolling bearings. Tribol. Int. 2014; 74:7–19. https://doi.org/10.1016/j.triboint.2014.01.023.

[59] Li, X., Guo, F., Poll, G., Fei, Y., Yang, P., Grease film evolution in rolling elastohydrodynamic lubrication contacts. Friction 2021; 9:179–90. https://doi.org/10.1007/s40544-020-0381-4.

[60] Greenwood, J.A., Elastohydrodynamic lubrication with Herschel-Bulkley model greases. ASLE Trans. 1972; 15:269–77. https://doi.org/10.1080/05698197208981427.

[61] Dong, D., & Qian, X., A theory of elastohydrodynamic grease-lubricated line contact based on a refined rheological model, Tribol. Int. 1988; 21(5):261–7. http://dx.doi.org/10.1016/0301-679X(88)90003-5

[62] Huang, L., Guo, D., Wen, S., Starvation and reflow of point contact lubricated with greases of different chemical formulation. Tribol. Lett. 2014; 55:483–92. https://doi.org/10.1007/s11249-014-0376-2.

[63] Hurley, S., Cann, P. M., IR Spectroscopic analysis of grease lubricant films in rolling contacts. Tribol. Ser. 1999; 36:589–600. https://doi.org/https://doi.org/10.1016/S0167-8922(99)80079-0.

[64] Hurley, S., Cann, P.M., Spikes, H.A., Thermal degradation of greases and the effect on lubrication performance. Tribol. Int., 1998. 31(9), 621-630. https://doi.org/10.1016/S0167-8922(98)00063-1

[65] Hurley, S., Cann, P. M, Spikes, H.A., Lubrication and reflow properties of thermally aged greases. Tribol. Trans. 2000; 43: 221–8. https://doi.org/10.1080/10402000008982332.

[66] Cen, H., Lugt, P.M., Morales-Espejel, G., Film thickness of mechanically worked lubricating grease at very low speeds. Tribol. Trans. 2014; 57:1066–71. https://doi.org/10.1080/10402004.2014.933936.

[67] Zhou, Y., Bosman, R., Lugt, P.M., An experimental study on film thickness in a rolling bearing for fresh and mechanically aged lubricating greases an experimental study on film thickness in a rolling bearing for fresh and. Tribol. Trans. 2019; 62:557–66. https://doi.org/10.1080/10402004.2018.1539202.

[68] Zhou, Y., Lugt, P.M., Tribology international on the application of the mechanical aging master curve for lubricating greases to rolling bearings. Tribol. Int. 2020; 141:105918. https://doi.org/10.1016/j.triboint.2019.105918.

[69] Cen, H., Lugt, P.M., Film Thickness in a grease lubricated ball bearing. Tribol. Int. 2019; 134:26–35. https://doi.org/https://doi.org/10.1016/j.triboint.2019.01.032.

[70] Cen, H., Lugt, P.M., Replenishment of the EHL contacts in a grease lubricated ball bearing. Tribol. Int. 2020;146. https://doi.org/10.1016/j.triboint.2019.106064.

[71] Shetty, P., Meijer R. J, Osara, J.A., Lugt, P.M. Measuring film thickness in starved grease-lubricated ball bearings: an improved electrical capacitance method. Tribol. Trans. 2022; 65:869–79. https://doi.org/10.1080/10402004.2022.2091067.

[72] Fischer, D., Mues, H., Jacobs, G., Stratmann, A., Effect of over rolling frequency on the film formation in grease lubricated EHD contacts under starved conditions. Lubricants 2019;7. https://doi.org/10.3390/lubricants7020019.

[73] Kaneta, M., Ogata T., Takubo, Y., Naka, M., Effects of a thickener structure on grease elastohydrodynamic lubrication films. Proc. Inst. Mech. Eng. Part. J. 2000; 214:327–36. https://doi.org/10.1243/1350650001543214.

[74] Kanazawa, Y., De Laurentis, N., Kadiric, A., Studies of friction in grease-lubricated rolling bearings using ball-on-disc and full bearing tests. Tribol. Trans. 2020; 63:77–89. https://doi.org/10.1080/10402004.2019.1662147.

[75] Kanazawa, Y., Sayles, R.S., Kadiric, A., Film formation and friction in grease lubricated rolling-sliding non-conformal contacts. Tribol. Int. 2017; 109:505–18. https://doi.org/10.1016/j.triboint.2017.01.026.

[76] Kochi, T., Sakai, M., Nogi, T., Dong, D., Kimura, Y., Experimental study on the physics of thick EHL film formation with grease at low speeds. Tribol. Lett. 2019;67. https://doi.org/10.1007/s11249-019-1166-7.

[77] Cann, P. M., Grease lubrication of rolling element bearings - role of the grease thickener. Lubr. Sci. 2007; 19:183–96. https://doi.org/10.1002/ls.39.

[78] Cann, P.M., Webster, M.N., Doner, J.P., Wikstrom, V., Lugt, P.M. Grease degradation in R0F bearing tests. Tribol. Trans. 2007; 5 0:187–97. https://doi.org/10.1080/10402000701261003.

[79] Cann, P.M.E., Chevalier, F., Lubrecht, A.A., Track depletion and replenishment in a grease lubricated point contact: a quantitative analysis. Tribol. Ser. 1997; 32:405–13. https://doi.org/10.1016/s0167-8922(08)70469-3.

[80] Cann, P.M., Spikes, H.A., In lubro studies of lubricants in EHD contacts using FTIR absorption spectroscopy. Tribol. Trans. 1991; 34:248–56. https://doi.org/10.1080/10402009108982033.

[81] Wilson, A.R., The relative thickness of grease and oil films in rolling bearings. J. of Mech. Eng. Sci., *10*(3), 253-260. 1968. https://doi.org/10.1243/JMES_JOUR_1968_010_003_01

[82] Dyson, A., Wilson, A.R., Film thicknesses in elastohydrodynamic lubrication of rollers by greases. Proc. I. Mech. E., Part J: J. Eng. Tribol., 188 (1), 33-44. https://doi.org/10.1243/PIME_PROC_1974_188_180_024

[83] Barz, M., Die Schmierfilmbildung in fettgeschmierten schnellaufenden Spindellagern. PhD thesis, Verlag nicht ermittelbar.; 1996.

[84] Jablonka, K., Glovnea, R., Bongaerts, J., Evaluation of EHD films by electrical capacitance. J. Phys. D. Appl. Phys 2012; 45. https://doi.org/10.1088/0022-3727/45/38/385301.

[85] Jablonka, K., Glovnea, R., Bongaerts. J., Morales-Espejel, G., The effect of the polarity of the lubricant upon capacitance measurements of EHD contacts. Tribol. Int. 2013; 61: 95–101. https://doi.org/10.1016/j.triboint.2012.11.016.

[86] Jablonka, K., Glovnea, R, Bongaerts J., Quantitative measurements of film thickness in a radially loaded deep-groove ball bearing. Tribol. Int. 2018; 119: 239–49. https://doi.org/10.1016/j.triboint.2017.11.001.

[87] Baly, H., Poll, G., Cann, P.M., Lubrecht, A.A., Correlation between model test devices and full bearing tests under grease lubricated conditions. Solid Mechanics and Its Applications 2006; ,134:229–40. https://doi.org/10.1007/1-4020-4533-6_16.

[88] Cen, H., Lugt, P.M., Effect of start-stop motion on contact replenishment in a grease lubricated deep groove ball bearing. Tribol. Int. 2021; 157:106882. https://doi.org/10.1016/j.triboint.2021.106882.

[89] Shetty, P., Meijer, R. J, Osara, J.A, Pasaribu, R., Lugt, P.M., Effect of grease filling on the film thickness in deep-groove ball bearings. Tribol. Trans. 2024; 67:62–9. https://doi.org/10.1080/10402004.2023.2282632.

[90] Shetty, P., Meijer R. J, Osara, J.A., Pasaribu, R., Lugt, P.M., Vibrations and film thickness in grease-lubricated deep groove ball bearings. Tribol. Int. 2024;193. https://doi.org/10.1016/j.triboint.2024.109325.

[91] Shetty, P., Meijer, R.J., Osara, J.A., Pasaribu, R., Lugt, P.M., Effect of bearing size on film thickness in grease-lubricated axially loaded deep groove ball bearings. Tribol. Int. 2024; 197. https://doi.org/10.1016/j.triboint.2024.109748.

[92] Huang, L., Guo, D., Liu X., Xie, G., Wan G.T.Y., Wen S., Effects of nano thickener deposited film on the behaviour of starvation and replenishment of lubricating greases Friction, 2016. https://doi.org/10.1007/s40544-016-0123-9.

[93] Hartl, M., Krupka, I., Poliscuk, R., Liska, M., Molimard, J., Querry, M., et. al. Thin film colorimetric interferometry. Tribol. Trans. 2001; 44: 270–6. https://doi.org/10.1080/10402000108982458.

[94] Hartl, M., Křupka, I., Radek, P., Liška, M., An automatic system for real-time evaluation of EHD film thickness and shape based on the colorimetric interferometry. Tribol. Trans. 1999; 42:303–9.

[95] Lakowicz, J.R., Principles of fluorescence spectroscopy Third Edition. New York 2006.

[96] Kostal, D., Onitsuka, S., Tanaka, H., Sugimura, J., Krupka, I., Hartl, M., Use of pyrene for quantitative fluorescence observation of Li-grease around EHL contacts. Tribol. Online 2020; 15:117–25. https://doi.org/10.2474/TROL.15.117.

[97] Jie, N., Zhang, Q., Yang, J., Huang, X., Determination of chromium in waste-water and cast-iron samples by fluorescence quenching of rhodamine 6G. Talanta. vol. 46. 1998. https://doi.org/10.1016/S0039-9140(97)00261-0

[98] Zhang, L., Xu, C., Li, B., Simple and sensitive detection method for chromium (VI) in water using glutathione-capped CdTe quantum dots as fluorescent probes. Microchimica Acta 2009; 166:61–8. https://doi.org/10.1007/s00604-009-0164-0.

[99] Okal, M., Kostal, D., Sperka, P., Krupka, I., Hartl, M., Effect of contact conformity on grease lubrication. Lubricants 2022; 10. https://doi.org/10.3390/lubricants10110289.

[100] Okal, M., Kostal, D., Sakai, K., Krupka, I., Hartl, M., Thickener behaviour in rolling elastohydrodynamic lubrication contacts. Tribol. Lett. 2024; 72. https://doi.org/10.1007/s11249-024-01874-0.

[101] Sugimura, J., Hashimoto, M., Yamamoto, Y., Study of elastohydrodynamic contacts with fluorescence microscope. vol. 38. Elsevier Masson SAS; 2000. https://doi.org/10.1016/S0167-8922(00)80165-0.

[102] SKF Rolling Bearings Catalogue 17000. 2018.

# LIST OF FIGURES

Fig. 1 A single deep-groove radial ball bearing. ..... 11

Fig. 2 Example of thickener microstructures (Lithium complex x Polypropylene thickener)[7] ..... 12

Fig. 3 The phases in the grease lubrication process [9] ..... 13

Fig. 4 Schematic representation of different types of grease behaviour during the churning phase [12] ..... 14

Fig. 5 Typical film thickness profile for an EHL line contact[15] ..... 16

Fig. 6 Difference of lubricant distribution in fully flooded and starved contact [28] ..... 17

Fig. 7 Dependence of the central film thickness in contact on the amount of lubricant before contact and ..... 18

Fig. 8 Decrease in film thickness due to increase in number of contact passes ..... 19

Fig. 9 Dependence of starvation level on SD parameter ..... 19

Fig. 10 Central film thickness decay in a starved circular EHL contact as a function of time. ..... 20

Fig. 11 Lubricant flow pattern around the EHL contact ..... 21

Fig. 12 Different lubrication states in different conditions [57] ..... 22

Fig. 13 Film thickness profiles for fresh and aged PU/E [65] ..... 23

Fig. 14 Grease film thickness variation inside a rolling bearing [65] ..... 24

Fig. 15 Effect of speed on film thickness and thickener concentration ..... 25

Fig. 16 Normalized film thickness in radial ball bearing ..... 26

Fig. 17 Effect of stopping on the development of film thickness in the bearing ..... 27

Fig. 18 Schematic representation of the link between methods and results ..... 36

Fig. 19 Ball-on-disc optical tribometer ..... 37

Fig. 20 Ball-on-ring optical tribometer ..... 38

Fig. 21 Scheme of the ball bearing test rig ..... 39

Fig. 22 Rheometer ..... 40

Fig. 23 The origin of optical interferometry at the disc-ball interface ..... 41

Fig. 24 Absorption and fluorescence emission spectra for anthracene [95] ..... 42

Fig. 25 Pyrene and Coumarin 6 fluorescence spectre ..... 43

Fig. 26 Diagram of the calibration assembly..... 45
Fig. 27 SEM images of grease thickener fibres..... 49

# LIST OF TABLES

Table 1 Specifications of rolling elements.[99] ..... 46

Table 2 Properties of used samples [99] ..... 47

Table 3 Properties of used samples [100] ..... 48

Table 4 Properties of used samples ..... 50